MODULATION OF BRAIN ACTIVITY BY WORKING MEMORY AND BY ANTIEPILEPTIC MEDICATION: A HIGH DENSITY EEG STUDY

By

SAHNG-MIN HAN

A DISSERTATION PRESENTED TO THE GRADUATE SCHOOL
OF THE UNIVERSITY OF FLORIDA IN PARTIAL FULFILLMENT
OF THE REQUIREMENTS FOR THE DEGREE OF
DOCTOR OF PHILOSOPHY

UNIVERSITY OF FLORIDA

2011

Dedicated to all my family and friends

ACKNOWLEDGMENTS

My most heartiest thanks go to my advisor, Dr. Mingzhou Ding, for giving me the research opportunity with his outstanding guidance, constructive criticism and generous support over the years. I deeply thank him for his infinite patience towards my whims and fancies so that I could pursue my research interests with great freedom.

I sincerely thank my committee members Dr. Thomas DeMarse, Dr. Linda Hermer and Dr. Hans van Oostrom for their support. A special thanks to Dr. Susan Marino and Dr. Jean Cibula for their endless advice and great collaboration in the drug study project. I am also very thankful to all my colleagues in the last and present. I only mention a few of them here: Dr. Anil Bollimunta, Dr. Rajasimhan Rajagovindan, Dr. Xianzhi Shao, Dr. Mukesh Dhamala, Dr. Yonghong Chen, Dr. Yan Zhang, Dr. Xue Wang, Dr. Hariharan Nalatore and Kristopher Anderson. I learned so much from the constructive discussions with them who brought great joy to my research. Tifiny and Kathryn, the BME staff, have been unbelievably helpful in processing my paperwork with big smile. Thanks to Art for resolving computer issues in time. I also thank all who participated in my experiments who made this research possible.

I owe what I am to my family and ancestors. Living alone and away from home made me realize how much I love them. I love my grandmother, my parents, older sister and relatives in Korea. Their lives always have been my best guiding light in life. I save my heartfelt appreciation for my wife who has shown genuine love, sacrifice and support during the last several years.

TABLE OF CONTENTS

page

LIST OF TABLES

LIST OF FIGURES

LIST OF ABBREVIATIONS

AED	Anti-Epileptic Drugs
ANOVA	ANalysis Of Variance
BNT	Boston Naming Tes
CA	Carbonic Anhydrase
CNS	Central Nervous System
COWAT	Controlled Oral Word Association Test
EEG	ElectroEncephaloGrams
EMG	ElectroMyoGram
EOG	ElectroOculoGram
ERD	Event-Related Desynchronization
ERP	Event Related Potential
ERS	Event-Related Synchronization
GABAA	Gamma-AminoButyric Acid A receptor
LTM	Long-Term Memory
MAPDS	Minnesota Adaptive Picture Description Stimulus
MCG	Medical College of Georgia
MVAR	MultiVAriate AutoRegressive
SALSA	System for Automated Language and Speech Analysis
SDMT	Symbol Digit Modalities Test
STM	Short-Term Memory
TPM	ToPiraMate

Abstract of Dissertation Presented to the Graduate School
of the University of Florida in Partial Fulfillment of the
Requirements for the Degree of Doctor of Philosophy

MODULATION OF BRAIN ACTIVITY BY WORKING MEMORY AND BY ANTIEPILEPTIC MEDICATION: A HIGH DENSITY EEG STUDY

By

Sahng-Min Han

May 2011

Chair: Mingzhou Ding
Major: Biomedical Engineering

It is estimated that in a given year in the US, there are 57.7 million people suffering from mental disorders (National Institute of Mental Health, 2010) and over 2.7 million from epilepsy (Centers for Disease Control and Prevention, 2008) with annual incidence of 50 per 100,000 persons (National Institute for Clinical Excellence, 2004). Some antiepileptic drugs used to treat epilepsy, have been associated clinically with adverse cognitive side effects (Meador, 1998). Between 11–20% of patients with refractory epilepsy report some type of cognitive adverse event when taking Topiramate (TPM) (Bootsma et al., 2004). While the pattern, and magnitude of adverse cognitive side effects have not been established for many classes of drugs because of, in large part, insufficient data recording facilities or inadequate research designs and analysis, the public health impact of these side-effects is enormous, considering that key human functions such as language and working memory are negatively affected. The severity of the problem is further magnified in more vulnerable populations such as the elderly. However, despite widespread use of drugs like TPM, the ability to predict which individuals are at risk for developing cognitive impairment has remained elusive.

Moreover, there are no clear clinical guidelines for physicians facing decisions involving the therapeutic management of cognitive side effects.

The aim of this dissertation was to investigate whether significant differences in TPM pharmacokinetics can account for a major portion of the inter-individual variability in effects of TPM on executive functions including working memory along with its key molecular mechanism and the age-old topic that is of much interest to neuroscientist but still remain debated: the functional role of alpha rhythm using our computational techniques. To do so, we first used a modified version of the Sternberg paradigm and verified the key behavioral findings of the original Sternberg task along with propagation of ERP separation latency and stronger Granger causality from frontal to visual area suggesting that information flows originated from the frontal executive structures.

After confirming the feasibility of the modified version paradigm, we applied the paradigm to TPM studies to investigate how behavioral performance and ERPs are affected by TPM. We used classical ERP method to analyze a recall period. The result revealed that (1) the more serum concentrations of TPM, the bigger the ERP difference and (2) frontal and left temporal areas were affected by TPM in the later memory processing stages.

Finally, we investigated how TPM modulates ongoing brain activity, particularly during the retention period of the working memory task. We applied Multivariate spectral analysis to calculate power and coherence and observed (1) the classical alpha power modulation pattern by working memory load, suggesting alpha oscillations can still be modulated by higher order executive processes despite the influence exerted on alpha by TPM and (2) the degree of alpha modulation by TPM is proportional to the TPM

serum level. (3) For the TPM condition, lower frontal-visual coherence value for the higher memory was observed. This may suggest that TPM may disrupt long distance communications between frontal and posterior areas.

Our approach would be an integration of the tools of clinical pharmacology, neurophysiology, linguistics, neuropsychology, bioinformatics and neuroscience into a multi-systems approach to account for, and eventually predict, how a drug's mechanisms of action in the brain and its disposition affect an individual's higher cognitive function. This approach will be significant because it will lead to well-designed studies that will advance our understanding of how drugs impair complex cognitive functions with greater precision and ecological validity than are presently available. Moreover, our methodology constitutes an improvement over existing population-based approaches that are insufficient to account for individual variation in response to treatment. In addition, this research will also provide a framework that can be used to advance our understanding of how drugs may enhance individual cognitive performance, thereby translating into the development of more effective and targeted drug therapies for epilepsy as well as other dementias, and cognitive disorders.

CHAPTER 1
INTRODUCTION

Human brain waves (electroencephalograms, EEG) were first recorded by Hans Berger in 1924 and neural oscillation in the 8 to 13 Hz range is referred to as the alpha rhythm (Berger, 1929). Despite 80 years of history since its discovery, the physiological mechanisms and function of alpha oscillations remain unclear (Berger, 1929; Shaw, 2003). Alpha rhythm was believed to be an 'idling' rhythm because prominent alpha activity can best be seen with their eyes closed during physical relaxation and relative mental inactivity (Berger, 1929). This idea is found to be no longer tenable. An emerging consensus is that for rejection tasks that require attention be paid internally (e.g. working memory and mental calculation), alpha increases as the level of attention increases (Ray et al., 1985; Cooper et al., 2003; Ray et al., 1985; Klinger et al., 1973; Schupp et al., 1994). A large body of data on enhanced alpha in internal attention tasks such as working memory places the functional role of alpha into a highly debated arena. There are currently two views on the function of enhanced alpha in working memory: 1) inhibition or disengagement of task irrelevant cortical areas and neuronal signals (Ray et al., 1985; Klimesch, 1996; Pfurtscheller, 2001; Pfurtscheller, 2003; Klimesch et al., 2007) and 2) neuronal representation of the information or direct involvement of memory process to maintain the information online (von Stein et al., 2000; Mima et al., 2001; Halgren et al., 2002; Palva et al., 2005; Palva et al., 2005). The alpha inhibition hypothesis assumes that small alpha amplitudes (known as event-related desynchronization or ERD) or desynchronized alpha activities reflect a state of high neuronal excitability, whereas large alpha amplitudes (known as event-related synchronization or ERS) or synchronized alpha activities reflect a state of inhibition.

This dissertation explores how ongoing alpha oscillation affects human working memory processing which is of much interest to neuroscientists for a long time. Further, we examine the electrophysiological effects of Topiramate (TPM), one of the most effective anti-epileptic drugs (AEDs), using the same working memory paradigm and the analytic techniques to support one of the most possible mechanisms of the drug and to address the cause behind the negative effects on human cognition. We have three specific aims.

Aim 1

To examine whether ongoing activity during the retention period of the working memory task was modulated by memory load. First we will verify and reproduce the key behavioral findings of the Sternberg paradigm by examining behavioral performance of healthy subjects. This will tell us whether the human memory scanning is serial or parallel and whether it is exhaustive or self-terminating process. Next we will examine whether we can find well known components such as P300 or any other components and to see whether these components are modulated by memory load by analyzing the ERP traces after the onset of the probe digit. Finally, we will apply multivariate spectral method to examine the power, coherence, and Granger causality during the retention period interval to assess the direction of information flow between neuronal ensembles in different brain regions so that we can add to our ability to better define the functions of complex neural networks in terms of alpha oscillation.

Aim 2

To investigate how behavioral performance and ERPs were affected by TPM. We will first examine behavioral and neurophysiological effects of topiramate while subjects performed the modified Sternberg working memory task. Specifically, we will look at

behavioral data in terms of response time (RT) and error rate. Then, dependence of behavioral measures and brain responses on the serum levels of TPM will be analyzed along with the body weight correlation. We further will examine the physiological basis of TPM's adverse effects on cognition by topographic activation and temporal (time course) plots by using the ERP method.

Aim 3

To investigate how TPM is modulating ongoing brain activity, particularly during the retention period of the working memory task. Specifically, we will first look at the resting state (with eye closed) where subjects were not involved in any mental task, making the period a simple, no confounding-factor state. Then, power and coherence modulations by memory load for all test conditions will be analyzed. We will also look at the relation between drug concentration and power modulation in different brain regions and compared the results with previous studies (Coulter et al., 1993; White et al., 1997; Gibbs et al., 2000).

CHAPTER 2
GENERAL METHODS

Parametric Multivariate Autoregressive (MVAR) Spectral Analysis

MVAR modeling is a parametric spectral analysis method in which time series models are extracted from the data and become the basis for deriving spectral quantities (Chen et al., 2006; Granger, 1969; Ding et al., 2006; Chen et al., 2006). The theoretical assumption of this method is that the EEG data from many trials can be treated as realizations of an underlying stationary stochastic process. One concern in this model is that the window size should be short enough to capture the non-stationary nature of fast changing neural activities.

The mathematical formulation can be briefly summarized as follows. Consider p channels of stationary stochastic process and we can denote it as

$$\mathbf{X}_t = (x_{1t}, x_{2t}, \cdots, x_{pt})^T, \tag{2-1}$$

where:

- T : Matrix transposition

Under general conditions the data can be expressed by a MVAR model

$$\sum_{k=0}^{m} A(k)X(t-k) = X(t) + A(1)X(t-1) + \cdots + A(m)X(t-m) = E(t) \tag{2-2}$$

where:

- *m*: Model order
- *E(t)*: Temporally uncorrelated residual error term with covariance matrix ∑
- *A(i)*: *p x p* Coefficient matrices

The MVAR model order m can be determined either by the Akaike Information Criterion (AIC) (Akaike, 1974) or Bayesian information criterion (BIC) (Schwarz, 1978). A(i) and covariance matrix Σ are obtained by solving Yule-Walker equations (Eq. 2-3) using the Levinson, Wiggins and Robinson (LWR) algorithm (Ding et al., 2000).

$$R(-k) + A(1)R(-k+1) + \cdots + A(m)R(-k+m) = 0 \tag{2-3}$$

Once an MVAR model is estimated with coefficients A(i) and covariance matrix Σ, (2-2) can be written in spectral domain

$$X(f) = H(f)E(f) \tag{2-4}$$

where:

- $H(f) = \left(\sum_{i=0}^{m} A(i) e^{-ij2\pi f} \right)^{-1}$ is transfer function. (2-5)

After ensemble averaging, spectral matrix can be evaluated as

$$S(f) = H(f)\Sigma H^{*}(f) \tag{2-6}$$

where:

- *: Matrix transposition and complex conjugation.

The power spectrum is the diagonal terms of the spectral matrix (Eq. 2-6) and ordinary coherence is the normalized off-diagonal terms. The coherence spectrum between two channels *l* and *k* is

$$C_{lk}(f) = \frac{\left|S_{lk}(f)\right|^2}{S_{ll}(f)S_{kk}(f)} \tag{2-7}$$

When the two channels are maximally interdependent, the value of the coherence spectrum (2-7) reaches 1 at frequency *f*. If they are independent to each other the value would be 0.

Bivariate Time Series and Pariwise Granger Causality Analysis

Granger Causality is a computational technique for evaluating the causal influence from one neural time series to another. Inspired by Wiener's idea (Wiener, 1956), Granger realized his prediction concept in linear regression models (Granger, 1969) and Granger causality is well defined in our MVAR model (Ding et al., 2006). Recent evidence suggests that Granger causality is a suitable technique for inferring the direction of neural communications directly from data. Multivariate autoregressive (MVAR) modeling provides a natural framework for incorporating the computation of Granger causality. The basic idea of Granger causality can be explained as follows.

Given two simultaneous time series:

$x_1, x_2, ..., x_n$

$y_1, y_2, ..., y_n$,

a linear prediction of x series using autoregressive model is:

$$x_n = a_1 x_{n-1} + a_2 x_{n-2} + \cdots + a_m x_{n-m} + \varepsilon_n \tag{2-8}$$

This is a univariate case of Eq. 2-2 and the model order, model coefficients and error term can be determined in the same way. Eq. 2-8 can be rewritten as in Eq. 2-9 when the previous values of the y series are included.

$$x_n = b_1 x_{n-1} + \cdots + b_k x_{n-k} + c_1 y_{n-1} + \cdots + c_k y_{n-k} + \eta_n \tag{2-9}$$

Based on Wiener's idea, Granger (Granger, 1969) formulated that

if $$\frac{Var(\eta_n)}{Var(\varepsilon_n)} < 1 \qquad (2\text{-}10)$$

then, the x prediction is improved by incorporating past knowledge of the y series and we say the y series has a causal influence on the x series. The x and y series can be reversed to predict the causal influence from x to y.

Geweke (1982) found a spectral representation of the time domain Granger Causality. Consider bivariate autoregressive model for two time series x_{1n} and x_{2n} then the Granger Causality spectrum from x_{2n} to x_{1n} is defined as

$$I_{2\to 1}(f) = -\ln\left(1 - \frac{\left(\Sigma_{22} - \frac{\Sigma_{12}^2}{\Sigma_{11}}\right)\left|H_{12}(f)\right|^2}{S_{11}(f)}\right) \qquad (2\text{-}11)$$

The logarithm is taken to preserve certain favorable statistical properties in Eq. 2-11 and the equation means that the proportion of x_{2n}'s causal contribution to the power of the x_{1n} series at frequency f. Indices 1 and 2 can be reversed to obtain the causality spectrum form x_{1n} and x_{2n} in Eq. 2-11. Geweke also showed that the integration of this spectral quantity over frequency is the time domain Granger causality and that the notion of the total interdependence between two time series x_{1n} and x_{2n} (Granger, 1969; Ding et al., 2006):

$$F_{1,2} = F_{1\to 2} + F_{2\to 1} + F_{1,2}$$

where:

- $F_{1\to 2}$, $F_{2\to 1}$: causal influences due to intrinsic interaction

- $F_{1,2}$: the instantaneous causality due to exogenous factors (e.g. a common driving input or volume conduction)

This Geweke's decomposition allows us to elucidate the causal influence between two time series.

Model Validation

There are a number of steps to validate the MVAR model after all model parameters are estimated (Ding et al., 2000; Chen et al., 2006)

(a) **Validating the suitable model order**: The MVAR model order can be determined either by the Akaike Information Criterion (AIC) (Akaike, 1974) or Bayesian information criterion (BIC) (Schwarz, 1978) and the statistical estimation should be robust against small model order variations.

(b) **The whiteness of the residual error:** The residual error should be white when the model has been well fit to the time series data (Ding et al., 2000; Lutkepohl, 1993).

(c) **Validation by other approaches;** As a cross validation, it is useful to recapitulate spectral quantities of the same data using other methods (Mitra et al., 1999) such as a conventional nonparametric technique based on discrete Fourier transform or a muti-taper spectral approach.

Interpretation

Given two simultaneously measured time series, one series has statistically causal influence to the other if we can better predict the second series by incorporating past knowledge of the first one (Wiener, 1956). This concept was later adopted and formalized by Granger (Granger, 1969) in the context of linear regression models of stochastic processes (Eq. 2-2). If the variance of the prediction error for the second time series at the present time is reduced by including past measurements from the first time series in the linear regression model, then the first time series can be called to have a causal (directional or driving) influence on the second time series. Reversing the roles

of the two time series, one repeats the process to address the question of causal influence in the opposite direction. So the flow of time plays an important role in determining directional causal influences from time series data. In this analysis, the EEG data represent numerous time series, and Granger causal influence is equated with the signal direction of synaptic transmission between neuronal structures.

Assessment of Statistical Significance

To assess the variability of the statistical quantities, we use a bootstrap resampling technique (Efron, 1982). It involves randomly sampling a pool of trials with replacement from the total ensemble, and then estimating the quantities of interest for this pool. Repeating this process many times for different pools of the same size we estimate the mean and standard deviation of any given quantity over the whole collection of estimated bootstrap values. The standard deviation gives a measure of the variability of the estimator (Ding et al., 2000). Significance testing can then be performed based on the resampling distributions.

For interdependence measures such as coherence and Granger causality spectra, we have adopted a random permutation approach (Brovelli, 2004) to build a baseline for statistical significance assessment. Consider two channels of recordings with many repeated trials. We can reasonably assume that the data from different trials are independent of one another. Randomly pairing data for channel 1 with data for channel 2 from a different trial leads to the creation of a synthetic ensemble of trials for which there is no interdependence between the two channels based on construction yet the temporal structure within a channel is preserved. Performing such random pairing with many different permutations will result in a distribution of coherence or causality spectra corresponding to the null hypothesis (i.e. distribution under the condition of no statistical

interdependence). Then the calculated value for a given statistic from the actual data is compared with this baseline null hypothesis distribution for the assessment of significance levels.

CHAPTER 3
EEG STUDY OF A MODIFIED STERNBERG WORKING MEMORY TASK

Backgrounds

Alpha Rhythm

The human brain contains hundreds of billions of neurons organized in networks. It is a source of a great amount of electrical oscillations, which are rhythmic changes in the level of depolarization and hyperpolarization in the dendritic and somatic membrane of neurons and can be reflected and captured on the scalp (Shaw, 2003). A German psychiatrist, Hans Berger was among the first to record some of those electrical oscillatory activities at the posterior surface of a human scalp that he named “alpha waves” (Berger, 1929) and later more refined definition from the International Federation for Clinical Neurophysiology (IFCN) is as follows : Rhythm at 8–13 Hz occurring during wakefulness over the posterior regions of the head, generally with maximum amplitudes over the occipital areas. Amplitude varies but is mostly below 50 μV in the adult… One comment is that the term alpha rhythm should be restricted to those rhythms that fulfill these criteria (Shaw, 2003).

Despite 80 years of history since its discovery, the physiological mechanisms of alpha oscillations remain not well understood (Berger, 1929; Shaw, 2003). As Hans Berger noticed, alpha rhythm is the most prominent activity in healthy humans and can best be seen with the eyes closed during physical relaxation and relative mental inactivity (Berger, 1929). These early findings lead to the idea that alpha oscillations are an ‘idling’ rhythm, representing a ‘calm yet alert’ brain state of the underlying cortex (Adrian, 1934). More recent evidence suggests that this idling hypothesis is untenable. An emerging consensus is that for sensory intake tasks such as sensory detection and

visual scanning, where attention is directed externally to detect environmental stimuli, alpha decreases as the level of attention increases (Ray et al., 1985; Cooper et al., 2003; Ray et al., 1985; Klilnger et al., 1973; Schupp et al., 1994). On the other hand, in rejection tasks that require attention be paid internally (e.g. working memory and mental calculation), alpha increases as the level of attention increases (Ray et al., 1985; Cooper et al., 2003; Ray et al., 1985; Klilnger et al., 1973; Schupp et al., 1994). A large body of data on enhanced alpha in internal attention tasks such as working memory places the functional role of alpha into a highly debated arena. There are currently two views on the function of enhanced alpha in working memory: 1) inhibition or disengagement of task irrelevant cortical areas and neuronal signals (Ray et al., 1985; Klimesch, 1996; Klimesch, 1997; Pfurtscheller, 2001; Pfurtscheller, 2003) and 2) neuronal representation of the information or direct involvement of memory process to maintain the information online (von Stein et al., 2000; Mima et al., 2001; Halgren et al., 2002; Palva et al., 2005; Palva et al., 2005).

The alpha inhibition hypothesis assumes that small alpha amplitudes (known as event-related desynchronization or ERD) or desynchronized alpha activities reflect a state of high neuronal excitability, whereas large alpha amplitudes (known as event-related synchronization or ERS) or synchronized alpha activities reflect a state of inhibition. In the neuronal representation hypothesis, enhanced alpha oscillation reflects an essential component of the neural network activity that sustains the neuronal representations of the information held online, whereas alpha suppression following stimulus onset reflects the termination of the memory process itself (Palva et al., 2007).

This view emphasizes the direct or indirect active role of alpha that is involved in memory processes.

Working Memory

Working memory refers to the mental ability to hold information across a relatively short period of time usually on the order of seconds for subsequent online manipulation of the information for higher cognitive functions (Baddeley, 1996). Previously, Atkinson and Shiffrin proposed a psychological model of human memory that consists of three components: Sensory memory (SM), Short-term memory (STM) and Long-term memory (LTM) (Atkinson et al., 1968). This multi-memory model explains the flow of memory process in the brain as in Figure 3-1. Incoming sensory information is stored in sensory memory for a very limited time period. Most of the input will be lost and only selected information by attention can be transferred from sensory memory into short-term memory (STM). This allows us to maintain information a little longer to use it for other ongoing task demands. Miller (Miller, 1956) has proposed that STM has a limited capacity of around seven items plus or minus two in case of alphabetic letters or number digits and called it the magical number seven. Peterson and Peterson have found that STM last approximately between 15 and 30 seconds (Peterson, 1959). LTM can retain information over much longer periods of time, from minutes to a lifetime and its capacity appears to have no limit. Information held in STM can be encoded into and retrieved from long term memory with the help of physiological processes yet to be identified. Memory in a very special occasion may also be transported directly from sensory memory to LTM when it receives a very strong attentional influence.

Baddeley developed the concept of working memory by integrating a large amount of works on short-term memory (Baddeley et al, 1996). In his working memory model, short-term memory was replaced with working memory which includes a temporal manipulation role along with a short-term maintenance of information. Originally, Baddeley & Hitch proposed (Figure 3-2A) that working memory contains one supervisory system called the central executive and two subsystems: the phonological loop and the visuo-spatial sketchpad. Later, Baddeley included a third slave system (Figure 3-2B): the episodic buffer. The central executive is a supervisory system that is responsible for integrating information from the slave systems and controlling the flow of information between the central and subsystems to facilitate cognitive processes.

The phonological loop in the above model is responsible for auditory or phonological information. Phonological information could be pure verbal form and visually encoded language components. Once the information comes to this system, it is stored in the phonological store and the articulatory rehearsal component repeats the auditory elements on a loop to keep them from decaying. The phonological loop is known to play an important role in learning a language (Baddeley et al., 1998). As the name indicates, the visuo-spatial sketchpad in the working memory model is thought to hold visual and spatial information, such as colors and shapes of objects or a certain location in the three dimensional space. Spatial information planning process (e.g. figuring out the shortcut to your destination) is also related to this system. The episodic butter is the newly added slave system to the working memory model in 2000. This system is believed to have links to LTM and integrate information from each slave system with time information to produce chronologically separated unit.

Objectives

In this chapter, 128 channels of scalp EEG (BioSemi, Amsterdam) were recorded from 10 healthy subjects performing a modified Sternberg working memory task. We first examined behavioral performance in order to verify and reproduce the key behavioral findings of the Sternberg paradigm. This step will tell us whether the human memory scanning is serial or parallel and whether it is exhaustive or self-terminating process. We further examined the ERP traces after the onset of the probe digit to see whether we can find well known components such as P300 or any other components and to see whether these components are modulated by memory load. Finally, we applied multivariate spectral method to examine the power, coherence, and Granger causality during the retention period interval to assess the direction of information flow between neuronal ensembles in different brain regions so that we can add to our ability to better define the functions of complex neural networks in terms of alpha oscillation.

Materials and Methods

Subjects

The experimental protocol was approved by the Institutional Review Board of the University of Florida. Ten subjects (ages 24−35, right-handed, 9 males, 1 rejected because of intentional negligence to respond correctly) were tested. Participants had normal or corrected-to-normal vision and reported normal neurological and psychiatric health. All participants pre-scanned for their performance using online simulator (refer to Appendix A) had 10−20 minute practice session and gave written informed consent prior to recording.

Experimental Paradigm

Subjects were shown a set of digits (0 to 9) on a CRT monitor for 1s, followed by a 3s retention period, which is followed by a probe digit. They were instructed to press a “yes” (index finger in the dominant hand) or “no” (middle finger) button to indicate whether the probe digit belonged to the set. Memory-load was controlled by the size of the digit set which in this experiment was chosen to be 1, 3 or 5. The main advantage of this paradigm over the classical Sternberg task is that, by presenting the items all at once rather than sequentially, the periods of encoding, retention and recall are all well separated in time so that it allows us to study both the temporal and spatial development of neural activity during the different stages of working memory process.

EEG Recording

128 channel scalp EEGs (BioSemi, Amsterdam) were recorded with a sampling rate of 1024 Hz. Four additional electrodes around the eyes recorded electrooculogram (EOG) to monitor horizontal (hEOG) and vertical (vEOG) eye movement. One electrode was attached to one of the arms depending on the hand orientation to check electromyogram (EMG). Seated in an acoustically and electromagnetically shielded chamber (ETS-Lindgren, Illinois), subjects were instructed to attend a CRT monitor (18 inch, located 107 cm from the ground and 1.2 m apart from the eyes) during recording. The experiment consisted of five blocks each containing approximately 60 trials lasting about 10 minutes. One minute of break time was given between blocks for the subject to relax and to reduce the fatigue effect. The whole experiment is about one hour in length. Subjects had a practice session until they felt comfortable with the task before the actual recording. They were monitored inside of the chamber through a closed-

circuit TV (CCTV) system for any necessary instructions through a wired radio system during the experiment.

Data Preprocessing

Data analysis was performed using BESA 5.2 (www.besa.de) and custom functions written in MATLAB 7.5 (www.mathworks.com). The raw EEG signal was band-pass filtered off-line from 0.1 to 30 Hz and downsampled to 200 Hz. Only trials with correct responses were considered for further analysis. In addition, trials with any of the following factors were excluded: (1) EOG exceeding 120 μV, (2) excessive muscle or movement artifacts, and (3) extreme response times (> 2.0 s or < 0.10 s). Table 2 presents the average trial rejection rate for each subject. The remaining artifact free signals were re-referenced against the average reference (Nunez et al., 1997; Ferree, 2006) and epoched from -100 ms to 800ms with 0 ms denoting the time of probe onset.

Behavioral and event related potential analysis

The behavioral performance was quantified by (1) reaction or response time (RT) defined as the time it took from the onset of probe digit to the key press response and (2) error rate defined as the ratio between the number of wrong trials divided by the total number of trials. After bad trials rejected, corresponding RT data were averaged for each load and study condition, then averaged across subjects. The event-related potential (ERP) was computed by averaging the epoched EEG segments elicited by probe stimuli for each memory load.

Spectral analysis: power , coherence and Granger causality estimation

The MultiVariate AutoRegressive (MVAR) time series modeling method was used to estimate power spectra (Ding, 2000) coherence and Granger causality. For alpha

frequency band analysis, power spectral densities (PSDs) were averaged over 8 to 13 Hz range then averaged across subjects for each channel.

Percentage change between load 5 and load 1 is defined by the following formula:

$$\frac{final - initial}{initial} \times 100$$

Channels in Regions of Interest (ROI) were selected where we can observe prominent changes in visual areas as in Figure 3-11A. The values from the selected channels were averaged and then averaged again across subjects. Coherence and Granger causality analysis follows the same procedure as in power estimation.

Significance Test

To provide statistical significance, the behavioral result was tested via a one way ANOVA. Post-hoc analyses were performed when necessary to evaluate the statistical significance for the difference between each load. Relative power data (Figure 5-3) obtained from two treatment sessions were tested using one-way ANOVA with a factor. In the ERP (Figure 3-8B), Granger causality (Figure 3-12) and coherence analysis (Figure 3-13), paired t-test were applied

Results

Behavior

Correct and incorrect response rates were calculated across all subjects to verify the behavioral performance. As shown in Table 3-1, subjects performed with low error rates and showed no distinct fatigue effect (Figure 3-5): later blocks did not show extended RTs compared to early blocks. The accuracy decreased about 2% as memory load increased from 1 to 5.

In order to check the comparable behavioral patterns, mean reaction time was calculated as a function of memory load. As can be seen from Figure 3-6, reaction time increased linearly as a function of the load which is consistent with the classical Sternberg task in which the digit to be remembered is presented one at a time. This supports the serial memory scanning hypothesis in which comparison occurs one item at a time. The slope of the function was 48 ms/digit which is slightly higher than the 38 ms/digit in the original task (Sternberg, 1966).

When a probe digit belongs to the memory set and a subject responds correctly then it is considered a positive response trial. When the digit does not belongs to the set and the subject responds correctly, it is considered a negative response trial. Figure 3-7 shows the mean reaction time for both positive and negative response trials. RT was faster for positive response trials than for negative response trials. This provides further support that the memory scanning process is serial.

ERPs

To test the functional role of frontal executives by memory load, the amplitudes of early components of probe-triggered ERPs were compared. The front-middle line channels were selected according as in Figure 3-12. As seen in Figure 3-8B, there was no significant amplitude differences in early stage ERP amplitude suggesting that it is not the sensory processing but the later memory processing stages that are controlled by the frontal executives. Thus the frontal executives are more involved in memory processing not the early cortical processing of the incoming stimuli.

Figure 3-10 shows the latency propagation defined by the onset of the amplitude separation in positive and negative response ERPs. We observed the linear trend in two different areas: (1) from the prefrontal to the middle of the brain ($r=0.81, p<0.01$) and (2)

from the middle to the visual area (*r=0.67 p=0.06*). There was no simple frontal to back propagation over the whole brain but the onset of the separation became delayed as it moves backward.

Power Analysis

Alpha band activity during the retention period was measured to evaluate whether and how memory load modulates neural oscillatory activity. EEGs from all 128 channels recorded during the interval from the onset of the memory set and to the onset of the probe digit were analyzed. Data were band-pass filtered from 1 to 55 Hz and the last two seconds of the retention period were extracted from each trial. Power spectra were calculated for each trial and then averaged for each memory load. Percentage power differences between load 1 and 5 were obtained for each subject and then grand averaged. As shown in Figure 3-11A, power enhancement was prominent over the parieto-occipital areas. The alpha enhancement for increased working memory or internal attention task is in line with previous reports (Ray et al., 1985; Cooper et al., 2003; Jensen et al., 2002; Ray et al, (1985); Busch et al., 2003; Sauseng et al., 2005). Dominant alpha band power over posterior areas might be generated by the alpha sources in the parietal-occipital fissure (Ray et al., 1985; Cooper et al., 2003; Jensen et al, 2002). As indicated earlier, the function of enhanced alpha is debated. It could be inhibiting the cortical areas not involved in the task. It could also reflect the representation of memorized items. As the number of items to be memorized increases, more neurons are recruited into synchronized networks to accommodate higher memory demand. Figure 3-11B shows the systematic increase in one of posterior areas taken from one of subjects.

Functional Connectivity

Granger causality (Chen et al., 2006; Granger, 1969; Ding et al., 2006; Chen et al., 2006) spectra from frontal to posterior and that in the opposite direction were derived to examine top-down effect and direction information during memory retention. Several frontal locations were selected around channel Fz, and posterior areas are represented by channels from posterior regions where high alpha activities were observed (Figure 3-11A). Granger causality were calculated for all possible pairwise combinations between frontal and posterior channels and averaged for those combinations then grand averaged across subjects. Coherence spectra were calculated in the same way. Granger causal influence from the frontal to the posterior regions were significantly higher for higher memory demand ($p=0.03$). No significant difference was observed in the opposite direction (Figure 3-12).

One possible interpretation of the increased frontal posterior driving is that it represents increased level of attention required for holding more information. It could also reflect the influence of the central executive controlling top-down working memory mechanism as postulated in Baddeley's working memory model. The exact underlying neurophysiological mechanisms remain to be understood. Coherence between the same frontal and posterior areas revealed no memory effect (Figure 3-13). The discrepancy between the two different spectral analysis methods may be due to the fact that coherence spectra can not distinguish the causal influences of both directions and it represents the combination of those directional information and exogenous factors such as volume conduction. It appears coherence spectra may not be a good connectivity measure in the present experiment.

Discussion

In this chapter we examined behavioral effects and brain oscillations in the scalp EEG of 10 healthy subjects performing a modified Sternberg task. First, we calculated mean reaction time (RT) as a function of memory load in order to verify and reproduce the key behavioral findings of the Sternberg paradigm. As shown in Figure 3-6, RT increased systematically as a function of memory load and the slope was 48 ms/digit which is slightly higher than the 38 ms/digit in the original task (Sternberg, 1966) but lower than similar experiment (64 ms/digit) (Jensen et al, 2002). These discrepancies may be due to differences in the experimental paradigms and well-performed subjects with very low error rates (Table 3-1) and no fatigue effect (Figure 3-5).

When RT is plotted as a function of memory load in the positive/negative set as in Figure 3-7, positive response trials were faster than negative ones (Sternberg, 1966: Sternberg, 1969: Sternberg,1975). This suggests a serial memory scanning in which each item is compared individually to the probe digit until either a match is made or the entire positive set is searched. Also, an exhaustive scanning process is assumed (Sternberg, 1975) because the function of both RTs has been found to increase at a similar rate (excluding low memory load which is load 1 in our experiment). If a self-terminating search process were the case, the positive response function, on the average, would increase at one half the rate of the negative response function assuming that only half of the positive set would have to be searched before a positive response could be made. Therefore, the entire set would have to be searched before a negative response could be made. The zero-intercept of the reaction time function is believed to reveal the latency of all processes other than the comparison process such as encoding time, response time (Roznowski, 1993).

Next, we examined the ERP traces during the recall period. Typical frontal ERP traces (Figure 3-8A) showed several trends: (1) no significant amplitude difference in early ERPs for different memory demands (Figure 3-8B). (2) the higher the memory load, the higher the amplitude (after 200 ms or more following the on set of the probe digit). (3) frontal negativity considered to be similar to FN400 (Rugg et al., 2007; Curran, 2000; Curran, 2007; Voss et al., 2010). Some studies have found P300 components in similar tasks proposing it as an index of multiple cognitive processes, including context updating or allocation of processing resources and decision-making (Polich, 2003; Polich, 2004; Polich et al., 1995; Berti et al., 2004; Braver et al, 2002; McEvoy et al., 2001; Schack et al., 2005). We, however, didn't see it but instead we observed FN400 often reported in familiarity-based recognition memory tasks (Rugg et al., 2007; Curran, 2000; Curran, 2007; Voss et al., 2010) Considering the fact that the simplest forms of testing for recognition is based on the pattern of yes-no responses where a subject has to indicate 'yes' if it is old or 'no' if it is a new item, FN400 component can be expected in our working memory paradigm.

We observed propagation of latency of separation in ERP analysis as seen in Figure 3-10. There is no simple frontal to back propagation over the whole brain but the onset of the separation between the positive and negative response ERPs became extended as it moves backward: prefrontal to middle of the brain and from the middle of the brain to the occipital area. This may indicate that information flows originated from the frontal executive structures.

Finally, we performed multivariate spectral analysis (power, coherence, and Granger causality) on the retention interval EEG data to assess the regional and the

inter-areal oscillatory synchronization and causal interaction between the fronto-occipital areas. We observed a clear alpha peak from the power spectra (Figure 3-11B) in the visual area and the alpha power increased monotonically with memory load which is similar to previous work (Ole 2002). This result supports the idea that in rejection tasks where attention is directed internally, such as working memory task, alpha activity increases with increase in attentional demand which is higher memory load in our experiment. There are some contradicting views on this alpha: increased alpha oscillation during working memory retention plays a direct role in maintaining the neural representation of the items held online (Palva and Palva 2007). But we believe this is unlikely to be the case given the recent evidence showing that increased alpha power occurs in parts of the brain not engaged in working memory maintenance (Jokisch and Jensen, 2007). And the alpha band Granger causality, summarized in figure 3-12, was increased for higher memory load (load 5) for Frontal→Occipital but no difference statistically for Occipital→Frontal. This increased alpha band Granger causality likely reflects increased top-down excitatory drive on local interneurons in visual cortex, leading to decreased cortical excitability and increased functional inhibition (Klimesch et al., 2007; Thut and Mimiussi 2009). Together with the ERP and alpha power and Granger analysis, we believe that the present study is providing a comprehensive understanding of attentional modulation of visual alpha oscillations as an inhibitory influence and their top-down control mechanism to implement the executive operations to facilitate information processing and decision-making (Driver and Frith 2000; Fuster 2005; Zhang and Ding 2009).

We note that the coherence between the same frontal and posterior areas revealed no memory effect (Figure 3-13). The discrepancy between the two different spectral analysis methods may be due to the fact that coherence spectra can not distinguish the causal influences of both directions and it represents the combination of those directional information and exogenous factors such as volume conduction. It appears Granger causality may be a better connectivity measure in the present experiment.

Table 3-1. Summary of behavioral data from ten subjects. All subjects performed the task well regardless of the size of memory load. Incorrect response rate is increased slightly for higher memory load.

Memory load	1	3	5
Number of trials	1000	1000	1000
Correct response (%)	98.90	98.40	96.60
Incorrect response (%)	1.10	1.60	3.40

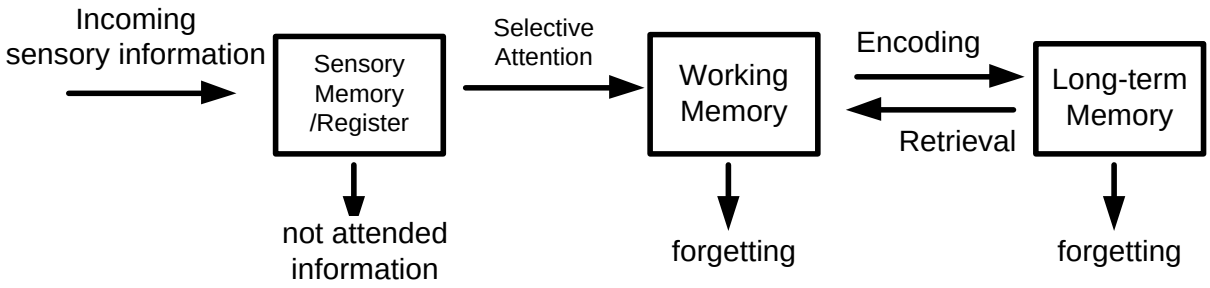

Figure 3-1. Atkinson and Shiffrin's memory model.

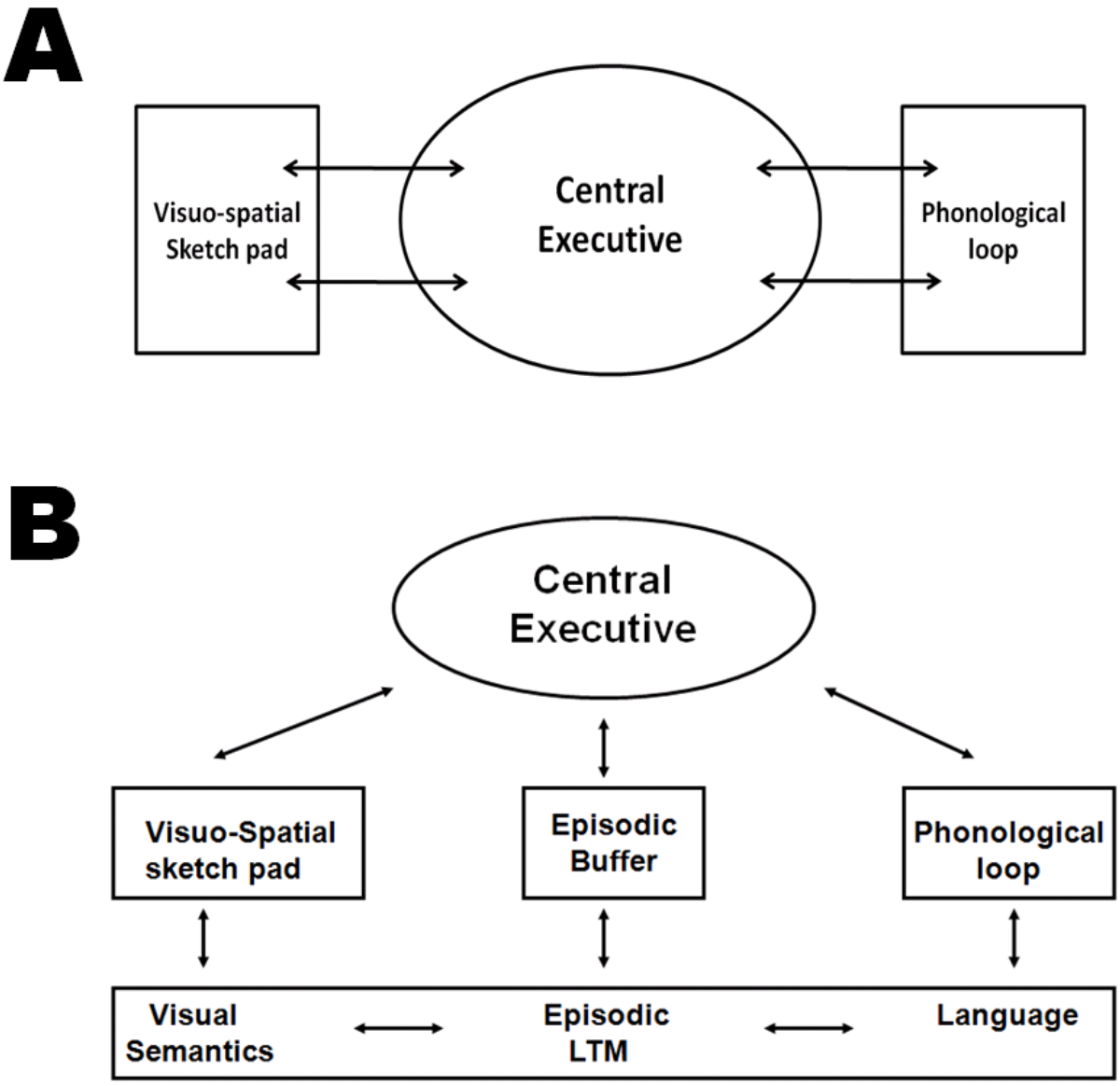

Figure 3-2. Working memory model proposed by Baddeley and Hitch. A) Original model. B) Updated model with episodic buffer.

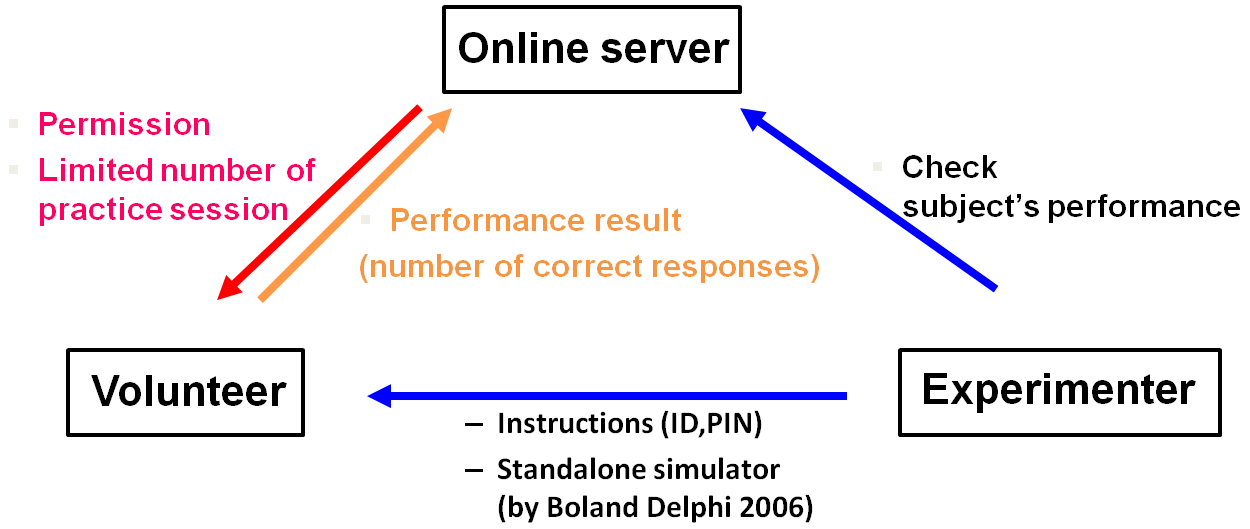

Figure 3-3. Diagram for the volunteer screening and training system.

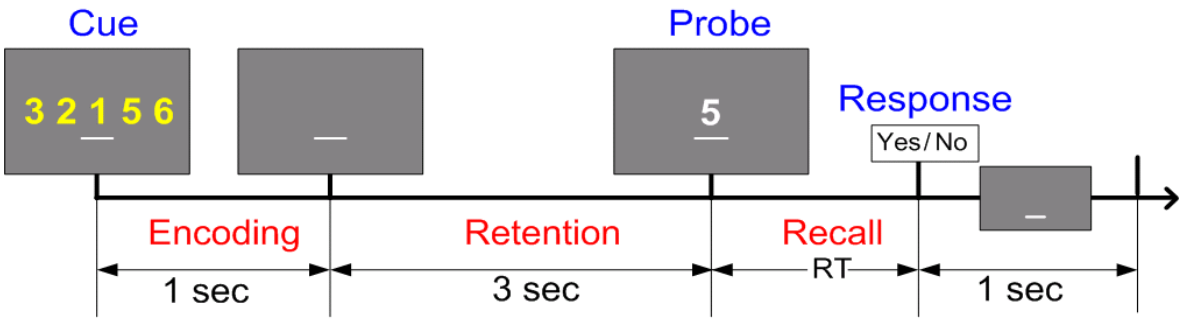

Figure 3-4. A modified Sternberg memory scanning paradigm.

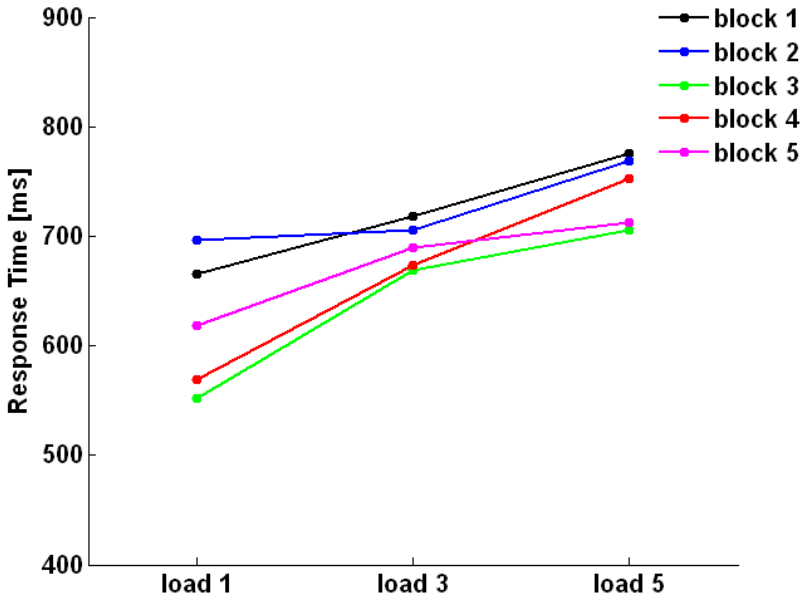

Figure 3-5. Mean response time as a function of memory load for all five blocks of recordings.

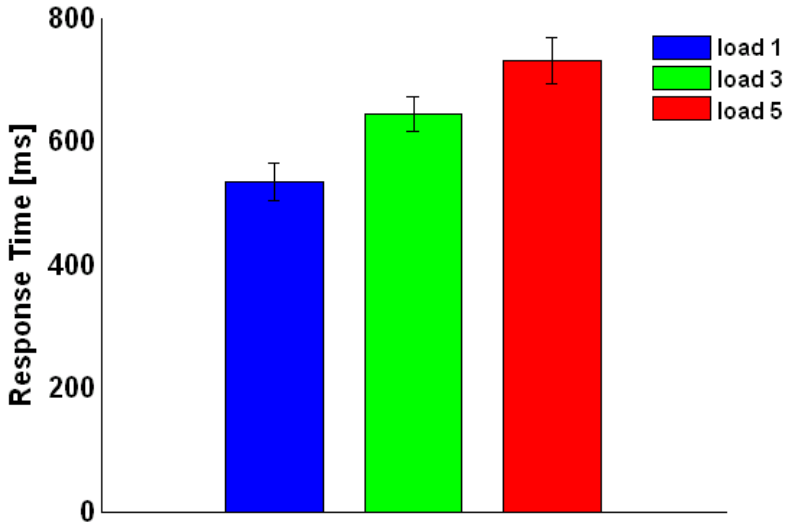

Figure 3-6. Mean response time to the probe digit as function of the memory load.

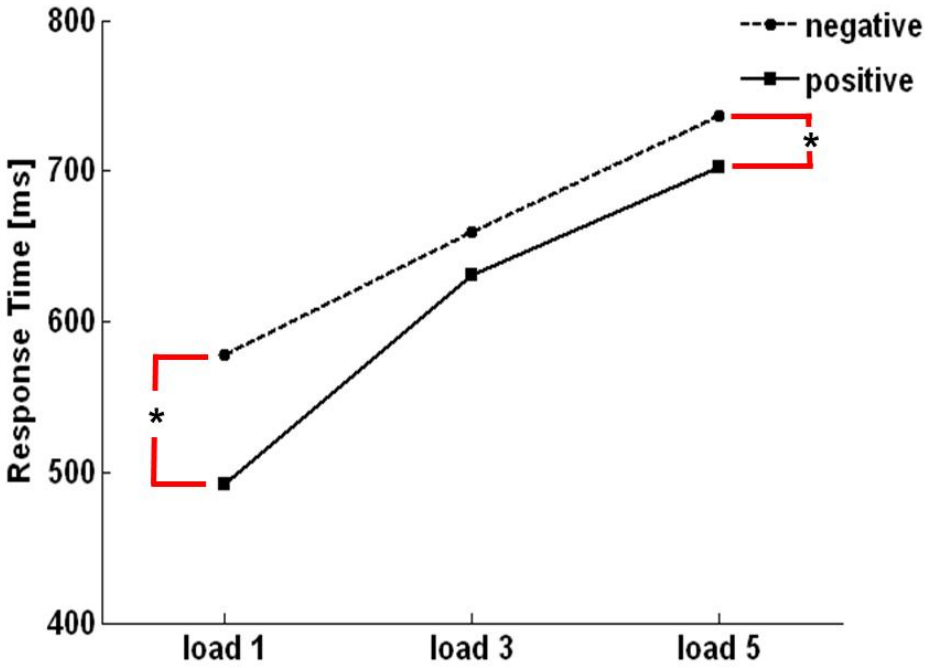

Figure 3-7. Mean reaction time for different trial types: positive and negative response trials. * $p < 0.05$ for both load 1 and 5 by paired t-test.

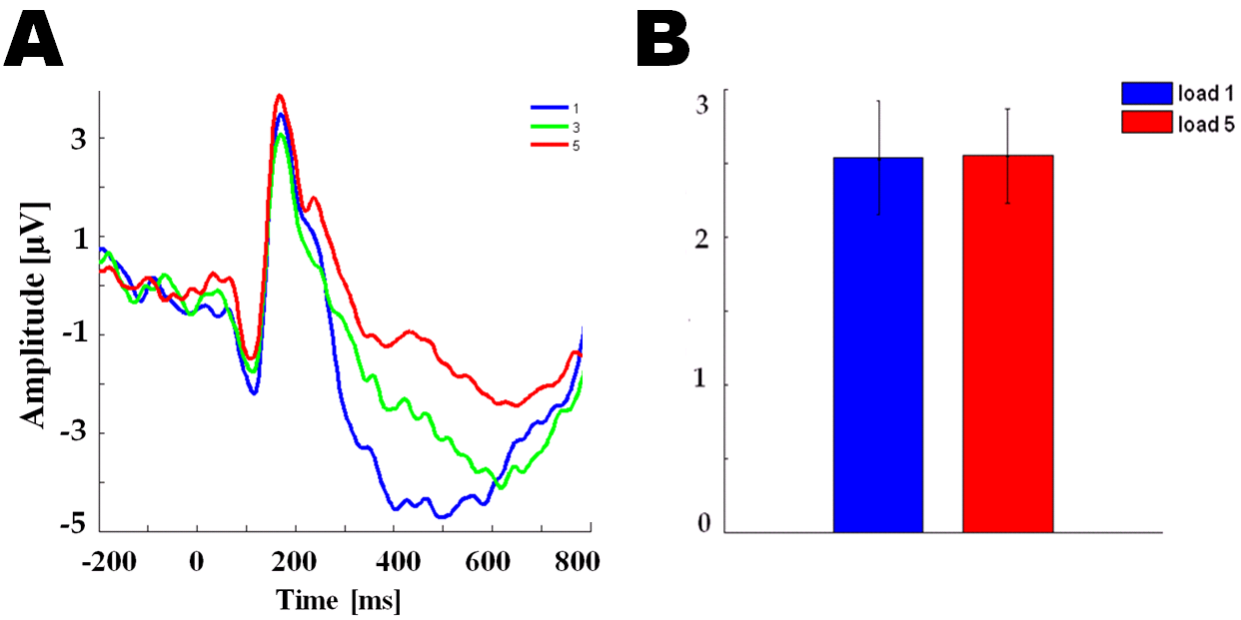

Figure 3-8. ERPs after the onset of the probe digits. A) Typical ERP traces from a frontal lobe electrode. B) Magnitude of early ERP with respect to memory load 1 and 5.

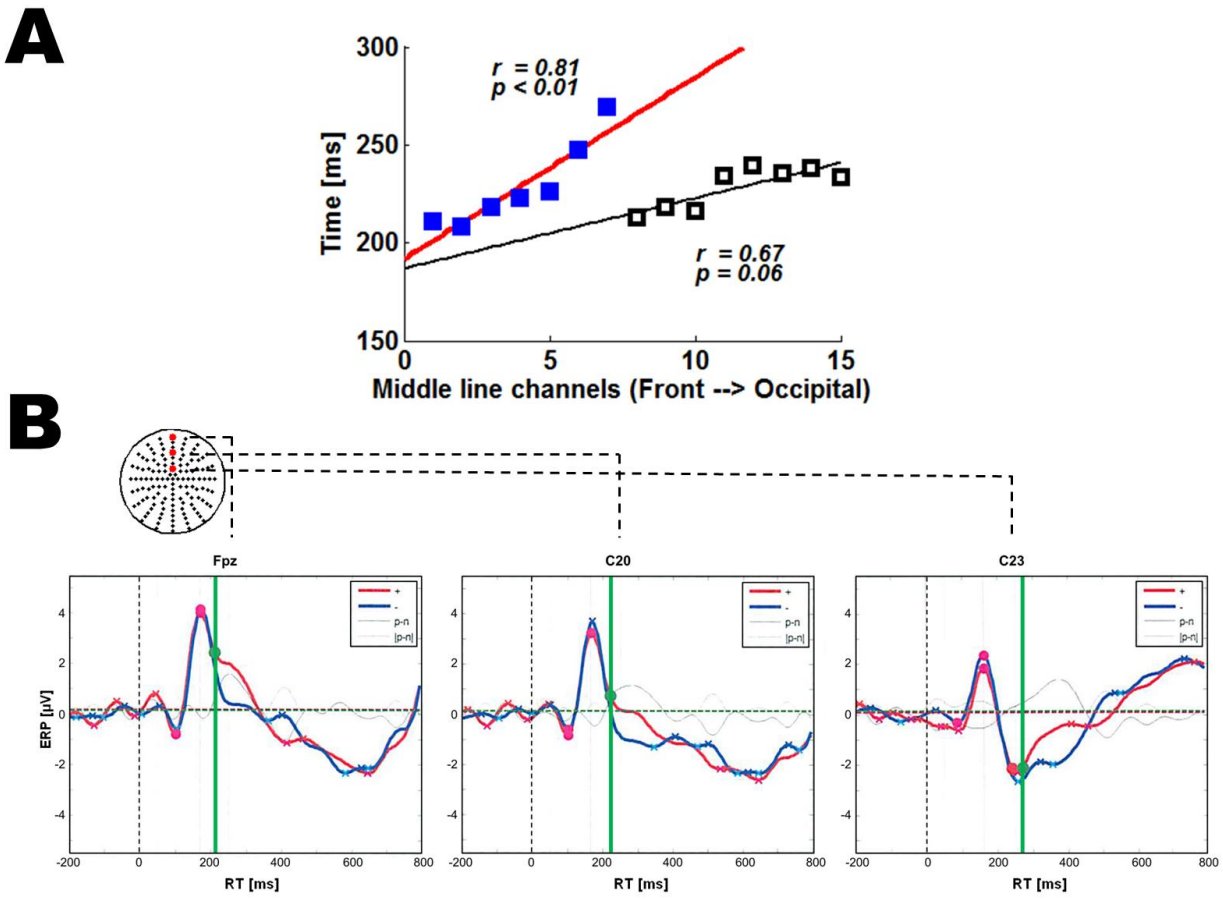

Figure 3-10. Propagation of latency of separations in ERP. A) Latency of the onset of the separation for middle line channels. B) The separation between the positive and negative ERPs from the frontal to occipital areas for load 3.

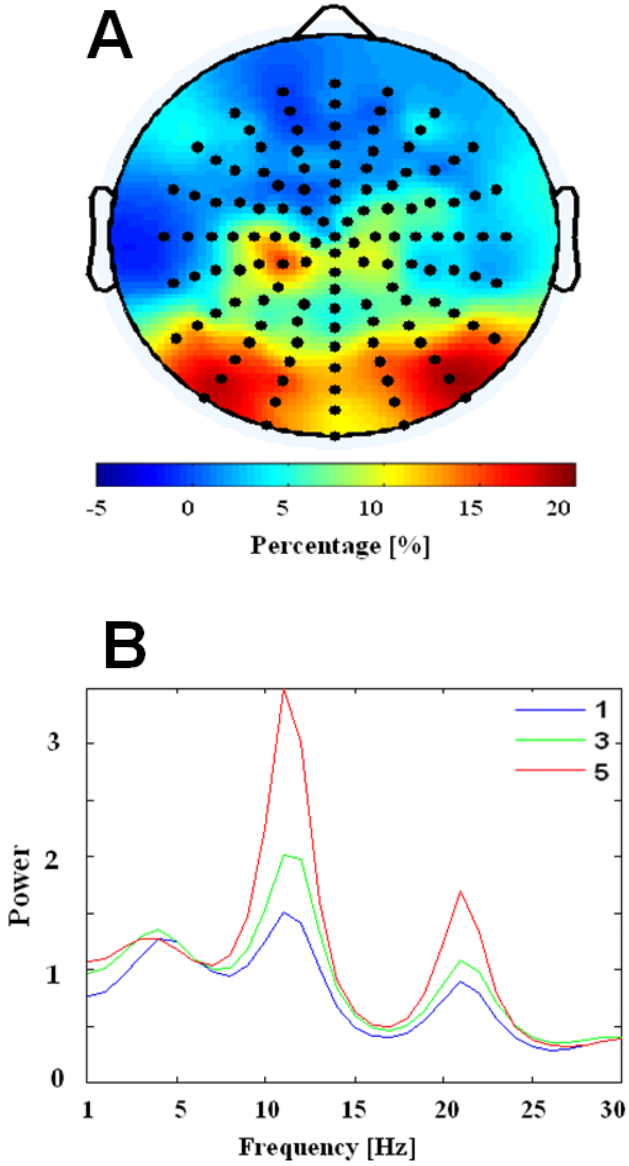

Figure 3-11. Power analysis. A) Topography showing regions of enhanced alpha power: load 5 versus load 1. B) Power specta from a posterior electrode showing systematic increase for three different memory loads.

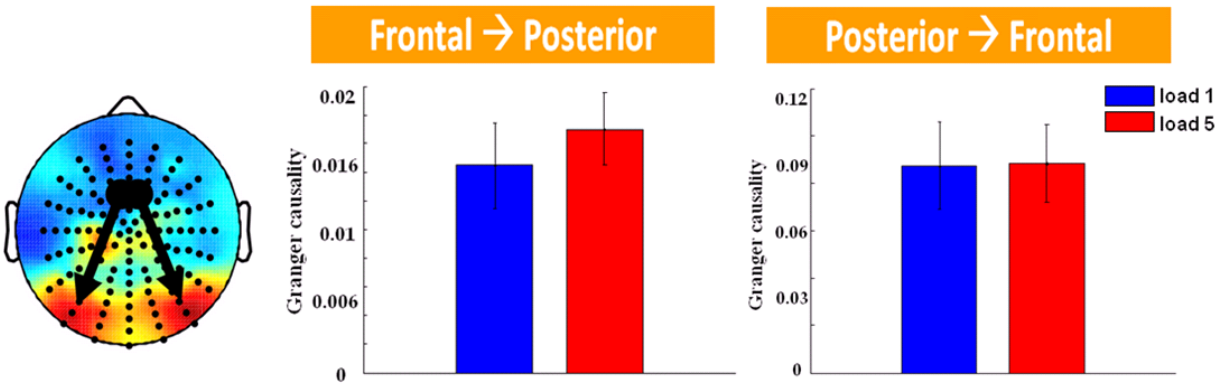

Figure 3-12. Granger causality in alpha band between fontal and posterior regions.

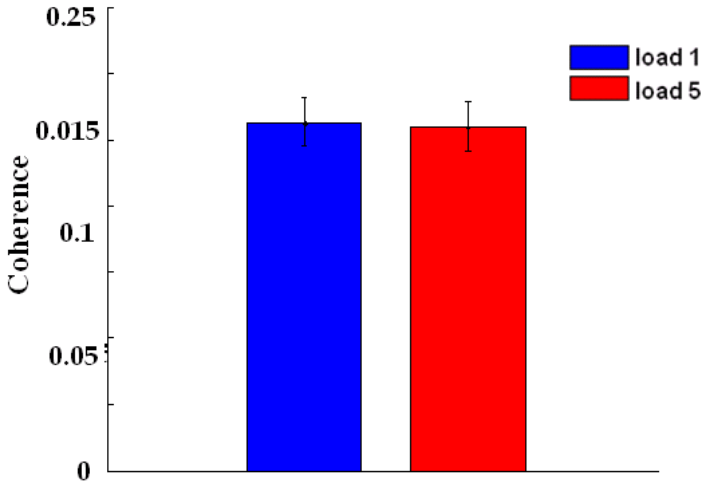

Figure 3-13. Coherence between fontal and posterior regions.

CHAPTER 4
EFFECTS OF ANTIEPILEPTIC DRUG ON HUMAN COGNITION: BEHAVIOR AND EEG ANALYSIS OF A WORKING MEMORY TASK

Backgrounds

Topiramate (TPM or TOPAMAX as a commercial brand name) (Figure 4-1) was discovered to have structural analogues of fructose-1,6-diphosphate that could inhibit the enzyme fructose 1,6-bisphosphatase (Shank et al., 2000). Compounds with this activity would inhibit gluconegenesis and thereby have potential as antidiabetic agents (Shank et al., 2000). In late 1979, TPM, as a second-generation AED (Sirven, 2007), was tested for aniticonvulsant activity in late 1979 and was found to possess multiple mechanisms of action (Shank et al., 2000; Langtry et al., 1997). Although this long-acting and relatively nontoxic drug has a wide spectrum of action and is effective in reducing seizure frequency (Shank et al., 1994) , it often induces intolerable adverse effects, predominantly related to the central nervous system including somnolence, psychomotor slowing, memory difficulty, attentional deficits, and speech problems (Aldenkamp, 2001; Aldenkamp et al., 1998; Devinsky, 1995; Massagli, 1991; Meador et al., 1995; Vermeulen et al., 1995; Martin et al., 1999). Studies conducted over recent years in patients and in healthy volunteers show that TPM induces dose-dependent effects on cognitive function with predominant language impairment (word fluency, verbal memory) (Aldenkamp, 2000; Aldenkamp et al., 2005; Aldenkamp et al., 2000; Meador et al., 2005; meador, 1997; Martin et al., 1999). The TPM-treated patients also reported loss of weight, paresthesias, dizziness, and nephrolithiasis (Mecarelli, 2001). Although numerous studies have investigated the clinical effects of TPM (including its efficacy in reducing seizures, and potential adverse events), few have focused on the

neuronal mechanisms of the cognitive deficits using physiological recordings such as electroencephalographic (EEG) data.

Our study addressed this problem. 100 mg of topiramate and placebo were administered randomly in a double blind fashion in two separate experimental sessions. Following a brief neuropsychological battery, all 128 channels of scalp EEG (BioSemi, Amsterdam) were recorded from subjects performing a modified Sternberg working memory task. Throughout this chapter, behavioral performance data combined with EEG activities recorded during topiramate sessions and those recorded during placebo sessions and during baseline sessions were compared. We examined behavioral and neurophysiological effects of topiramate while subjects performed the modified Sternberg working memory task. Specifically, we first looked at behavioral data in terms of response time (RT) and error rate. Then, dependence of behavioral measures and brain responses on the serum levels of TPM were analyzed along with the body weight correlation. We further examined the physiological basis of TPM's adverse effects on cognition by topographic activation and temporal (time course) plots by using the ERP method.

We note that, in contrast to previous AED studies where only a few recording channels were used and the focus was on a couple of ERP components (Nuwer, 1997; Flink et al., 2002; Stokes et al., 2004 Smith et al., 2006; Jung et al., 2010), in our ERP study 128 channels were utilized to map activities across the whole brain. As a result we can discover the target brain regions that are directly related to the drug's cognitive dysfunction. Our topographic and temporal neuro-electrophysiologic approach may one day provide some clinical insights for physicians facing decisions involving the

therapeutic management of cognitive side effects of TPM. Further, our work can open a new chapter by accelerating significant interactions between different areas: clinical pharmacology, linguistics, engineering, and neuroscience.

Materials and Methods

Subjects

Eleven volunteers who reported normal neurological and psychiatric health with normal or corrected-to-normal vision gave written informed consent and participated in the study. The experimental and recording protocol was approved by the Institutional Review Board (IRB) of the University of Florida and the affiliated Shands Hospital at UF. Of the eleven subjects initially enrolled, two were excluded: one was suspected of drug abuse and the other did not finish all the required recording sessions. Data from the remaining nine subjects (mean age 22 ± 2 years, 2 females, all right-handed) were included in the analyses reported here. The 2 female subjects underwent an additional test for pregnancy and the result was negative. All subjects were asked to abstain from alcoholic beverages or over-the-counter medications for at least 48 hours prior to testing though they were permitted to consume caffeinated beverages on the day of their assessment if that is part of their standard daily routine.

Experimental Design Overview

This is a double-blind, placebo-controlled study. Subjects were required to carry out four separate visits (Table 4-1). The first visit provided the baseline condition. On the 2^{nd} and 3^{rd} visits, after vital signs check by a physician or a registered nurse, the participants were given either a single dose of 100 mg of TPM orally or placebo according to a randomization schedule maintained by the UF Research Pharmacy. A period of one hour and 30 minutes was allowed to elapse before the subjects underwent

a neuropsychological battery and performed the working memory task during which EEG was recorded. At the end of the experiment blood samples (10 mL) were collected. Two weeks after the 3rd visit, the subjects came back for a post-study session, where they took the neuropsychological battery only.

Neuropsychology Battery

A battery of neuropsychological tests that measures language-specific cognitive processes was administered (Table 4-2.): Medical College of Georgia (MCG) test; referred to as a 'discourse-level' memory test since it requires the retelling of a narrative, rather than a list of words, like most other recall tests require. Symbol Digit Modalities Test (SDMT), a test of graphomotor and psychomotor speed (Smith, 1968), a test which primarily assesses complex scanning and visual tracking (Shum et al., 1990) with the added advantage of providing a comparison between visuomotor and oral responses. SDMT scores also correlated significantly with neuroradiologic evidence of caudate atrophy in Huntington patients (Starkstein et al., 1988). Pfeffer and his colleagues (1981) found the SDMT to be the "best discriminator" of dementia and depression our of a set of eight tests, which included the Trail Making Test plus tests of immediate and short-term memory, reasoning, and motor speed; Controlled Oral Word Association Test (COWAT) which measures the ability to generate words beginning with a specific letter of the alphabet such as F, A, S. Subjects initial responses is known to depended on rapid access of words from semantic memory with very little effort, while late productions depended on strategies for effortful searching of semantic memory and this test has proven to be a sensitive indicator of brain dysfunction. Frontal lesions, regardless of side, tend to depress fluency scores, with left frontal lesions resulting in lower word production than right frontal ones (Miceli et al., 1981; Perret, 1974; Ramier

et al., 1970). Category Fluency, in which the subject lists as many names (e.g., of animals, of boy's names) as they can in one minute is known for detecting people with an impairment usually attributed to a break down in semantic knowledge about categories (Monsch et al.,1994); Category Switching, where the subject switches between recall of names from two different categories (e.g., between fruits and furniture); Action Verb Fluency, in which the subject lists as many action verbs (e.g., eat, swim) as they can in one minute where patients with dementia show disproportionate difficulty; Boston Naming Test (BNT), which measures the ability to name objects from line drawings; This test effectively elicits naming impairments in aphasic patients (Margolin et al., 1990). Although this test was designed for the evaluation of naming deficits, Edith Kaplan recommends using it with patients with right hemisphere damage, too. The BNT is also widely used in dementia assessment as a sensitive indicator of both the presence and the degree of deterioration. Minnesota Picture Description test (or Minnesota Adaptive Picture Description Stimulus: MAPDS).in which the subject is asked to describe a black-and-white schematic pencil drawing or a full color of a scene containing several types of elicitation stimuli. This is designed specifically for studies to minimize practice effects over multiple visits while keeping the complexity and thematic content of the stimuli approximately constant. This test is administered immediately after the other standard picture description task (Refer to Appendix B) and relied on a series of computer generated household scenes controlled for the number of scene participants. Administration of this battery took approximately 30 minutes. All tests were audio-taped using stereo SUMA microphone (Andrea Electronics Co., New York) for further speech and language analysis by the Minnesota group who has developed the

System for Automated Language and Speech Analysis (SALSA) to precisely and objectively identify the effects of TPM administration on language. The result will be discussed in their forthcoming paper.

Working Memory Paradigm

The subject performed a modified Sternberg visual working memory task which is the same as that used in Chapter 3. Briefly, at the beginning of each trial, they were shown a set of digits (0 to 9) on a CRT monitor for 1s, which was followed by a 3s retention period. At the end of the retention period, a probe digit appeared, to which they responded by pressing a “yes” (index finger in the dominant hand) or “no” (middle finger) button to indicate whether the probe digit belonged to the set. Memory-load was controlled by the number of digits (1, 3 or 5) in the memory cue. The paradigm consists of seven blocks of trials with 60 trials per block. The digits and the memory loads are equally likely to occur. For each memory load a total of 140 trials were performed. A practice block was given before testing to familiarize the subjects with the task. During recording, one-minute breaks were inserted between blocks to reduce the effect of possible fatigue.

Data Acquisition

The electroencephalogram (EEG) recording was conducted in an acoustically and electrically shielded chamber (ETS-Lindgren, Illinois) in the Neuroinformatics Lab in the J. Crayton Pruitt Family Department of biomedical Engineering at the University of Florida. Seated on a non-metal wooden chair in the chamber, subjects were instructed to attend a CRT monitor (18 inch) which was located approximately 107 cm from the ground and 1.3 m from the eyes). The scalp EEG data was recorded with a 128-channel BioSemi ActiveTwo System at a sampling rate of 1024 Hz. In addition, six additional

flat-type electrodes were used: (a) two on each lateral side of both eyes to monitor horizontal electroculogram (hEOG), (b) two above and below the left eye to monitor vertical eye movement (vEOG), and (c) two on the left and right sides of preauricular points. The working memory paradigm was delivered by a custom program written in BeriSoft Experimental Run-Time System (ERTS) language, and the key press response was registered by an EXKEY microprocessor logic pad (http://www.berisoft.com), both running under MS-DOS. In addition to the working memory experiment, one minute of ongoing EEG activity was also recorded for both eye-closed and eye-open state before the main task.

Blood Samples

All subjects have been prescreened for co-medication interactions. Safety data will be collected at each study visit. The attending physician (Jean Cibula, MD or the study registered nurse) collected and monitored safety data during drug administration. Before study drug administration, a baseline BP (blood pressure) and heart rate were collected and recorded. MD performed a brief physical and neurological examination to determine baselines. Post-administration, vital signs were checked and recorded. After completing the EEG recording session, Subjects' blood samples were drawn for serum concentrations using the blood sample kits (Minneapolis, MI). Subject DNA were also extracted for those who consent. All analyses were performed at the University of Minnesota Center for Clinical and Cognitive Neuropharmacology. Genotyping of SNPs (single nucleotide polymorphisms) of interest was done using a method based on PCR amplification of the region containing the polymorphism. Data was analyzed with the Sequencer software package, and the genotypes called and entered into an Excel spreadsheet. Another method for in-house validation of novel SNPs is to PCR amplify

the product and digest it with a restriction enzyme whose recognition site is altered by the SNP, rending digestion patterns upon gel electrophoresis that clearly reveal the individual's genotype. In addition, pyrosequencing and TaqMan method were utilized for higher throughput. Drug metabolism and response genes were analyzed. SNP choice will be based on estimated allele frequency in the subject population, putative effect of the polymorphism on protein function, prior availability in a commercial assay (e.g. TaqMan system), and ability to deduce haplotype information. University of Minnesota applied a chip-based platform that allows genotyping of hundreds/thousands of SNPs at one time.

Data Preprocessing

Data analysis was performed using BESA 5.2 (www.besa.de) and custom functions written in MATLAB 7.5 (www.mathworks.com). The raw EEG signal was band-pass filtered off-line from 0.1 to 30 Hz and downsampled to 200 Hz. Only trials with correct responses were considered for further analysis. In addition, trials with any of the following factors were excluded: (1) EOG exceeding 120 μV, (2) excessive muscle or movement artifacts, and (3) extreme response times (> 2.0 s or < 0.10 s). Table 2 presents the average trial rejection rate for each subject. The remaining artifact free signals were re-referenced against the average reference (Nunez et al., 1997; Ferree, 2006) and epoched from -100 ms to 800ms with 0 ms denoting the time of probe onset.

Behavioral and Event Related Potential Analysis

The behavioral data was analyzed via a 3 X 3 factorial ANOVA with memory load as a factor and the three experimental sessions (baseline, drug, and placebo) as treatment levels. Post-hoc analyses were performed when necessary to evaluate the statistical significance for the difference in behavioral measures over memory loads or

drug conditions. The visual event-related potential (ERP) was computed by averaging the epoched EEG segments elicited by probe stimuli for each memory load for all drug conditions. To compare the difference between two drug conditions (either TPM and placebo or TPM and baseline), the ERP difference were transformed into Z scores using the following formula, which take into account the intrinsic variability between the two ERP traces by incorporating the ERP differences during the prestimulus period. Then topographic activation and temporal (time course) plots were generated using the converted Z score.

$$\mathbf{Z} = \frac{\mathbf{X} - \boldsymbol{\mu}}{\boldsymbol{\sigma}}$$

Where:

- X: Difference waveform between the TPM and placebo grand averaged ERPs for 0ms to 800ms
- μ: Mean of the difference waveform in the prestim period, -100ms ~ 0ms
- σ: Standard deviation of the difference waveform in the prestim period

Results

Behavior

The subjects performed the task according to instructions. As shown in Fig. 4-3A, subjects responded faster and more accurately for lower memory load across all treatments. Topiramate tended to increase subjects' reaction time and error rate. The 3 x 3 factorial ANOVA found that RTs were significantly affected by both the memory load ($F_{2,72}$ = 12.6, p < .001) and experimental treatment ($F_{2,72}$ = 6.8, p = .002) but there was no significant interaction between the two factors ($F_{4,72}$ = 0.16, p = 0.96). Tukey HSD (honestly significant difference) pair-wise comparisons indicated that RT was

significantly longer for higher memory load ($p < .001$ for load 5, and $p = .027$ for load 3) when compared to lower memory load (load 1). Significant differences were also observed when comparing TPM treatment to all other treatment types ($p = .003$ for placebo, and $p = .016$ for baseline). Response error rate data was also subjected to a separate three-way ANOVA with factors of drug condition and memory load and a subsequent post-hoc analysis. Error rate was significantly higher after TPM treatment relative to placebo condition ($p = .037$). Although no statistical difference in error rate was found between memory loads, a trend could be identified: the higher the memory load, the more errors the subjects tended to make.

Percentage RT differences between TPM and placebo conditions for all memory loads were plotted as a function of each individual's TPM concentration level in blood. The Spearman's rank correlation coefficient (SRCC) was positive across memory loads but did not reach significance ($r = 0.40$, $p = 0.29$; $r = 0.62$, $p = 0.09$; $r = 0.47$, $p = 0.21$ for load 1, 3, 5 respectively) as depicted in Fig. 4-3B. A negative correlation was found (Figure 4-3D) between the TPM concentration level and the body weight and SRCC was improved from $r = -0.33$ ($p = 0.39$) to $r = -0.74$ ($p = 0.04$) when an outlier was excluded. Figure 4-6 shows TPM and baseline comparison for the drug's plasma level correlation with percentage RT differences by Spearman's rank correlation coefficient (SRCC). Positive trend was stronger than those of placebo comparison for all memory load and the Spearman's rank correlation coefficient was improved to $r=0.86$ ($p=0.01$) for load 5 without outlier.

ERPs

Event -related potentials from representative electrodes (memory load 5) are presented as grand average waveforms in Figure 4-4 for TPM and placebo conditions.

Visual inspection suggested that the TPM and placebo waveforms began to show prominent separation around 400 ms in frontal (FPz) and middle left (C3) regions. Difference in the two grand averaged ERPs for TPM and placebo conditions were transformed into Z scores to incorporate the intrinsic variability between the two ERP traces and their traces (Figure 4-5A) from selected channels emphasized the difference between the two ERPs in the frontal and left region as expected.

Z area defined as the sum of the integral of z score curve in the interval from 0 to 800 ms for all 128 channels computed for each memory load and shows larger area in higher memory load. This led us to analyze data for load 5 where the larger difference was found between TPM and placebo conditions. Time course plots of the Z score (Figure 4-5C) reveals the temporal information that the significant differences between TPM and placebo-related ERP begin to emerge after around 400 ms. The difference were considered significant when it met the following criteria.

1) The difference should be continuous for at least 60ms
2) The difference should not less than the threshold which is defined by

$$\text{threshold} = M + 3 \times \sigma$$

where:

- M: Mean of z score for each channel
- σ : Standard deviation of z score for each channel

Topographic z score amplitude map (Figure 4-5D) averaged over 100ms time block each and the frontal and left region of the brain shows prominent separation which is similar to grand averaged ERPs (Figure 4-4) and temporal analysis (Figure 4-4C).

Figure 4-7A shows TPM and baseline ERP comparison for selected frontal channels. Eight subjects (an outlier was excluded) were grouped into three according to their ERP difference magnitudes (ERP differences were calculated for each time points from 200 ms to 800 ms and then added together). These three ERP groups were correlated with TPM concentration and showed strong positive trend: the more serum concentrations of TPM, the bigger the ERP difference.

Discussion

In this chapter we examined behavioral and neurophysiological effects of Topiramate using a modified Sternberg working memory test. TPM significantly increased subjects' reaction time and error rate. This is in line with many other TPM studies where it has been shown that TPM (with high or low doses) causes cognitive impairments in either patients or healthy volunteers (Aldenkamp, 2000; Aldenkamp et al., 2000; Blum et al., 2006; Dodril, 1988; Lee et al., 2003; Lee et al., 2006; Martin et al., 1999; Meador et al, 1991, 1995A, 1995B, 2001A, 2001B, 2003, 2005A, 2005B; Salinsky, 2003; Salinsky et al., 2002A, 2002B, 2003, 2004, 2007; Thompson et al., 2000). One of our main findings is the dependence of behavioral measures and brain responses on the serum levels of TPM provided by the Minnesota group. The levels of TPM plasma concentration are consistent with previous clinical studies: although topiramate is known to be rapidly absorbed (Easterling et al., 1988; Perucca, 1997), when administered as monotherapy, topiramate is not extensively metabolized and 70–80% of an administered dose eliminated unchanged (Rosenfeld, 1997; Langtry et al., 1997; Laurence et al., 2008; Perucca, 1997) and has a mean peak plasma concentration of 25.8 μg/mL after about two hours administration at steady state in patients with epilepsy (Sachdeo et al., 1996). We found a negative correlation between the TPM concentration

level and the body weight which supports one of topiramate's pharmacokinetic properties in humans: TPM distribution appears to be distributing into a volume that approximates total body water (Streeter et al., 1995). It is known that the heavier the people, the more body water they have. So people with more weight might dissipate or metabolize the drug more effectively.

In the analysis of the relationship between TPM level and behavioral performance (RT differences between the drug and placebo/baseline conditions) we found they are positively correlated. This finding supports a previous study showing that the mean topiramate concentrations in patients with impaired CNS functions were significantly higher than those in patients without side effects (Reife et al., 1995). This result is significant because the correlation between drug concentration and behavior performance demonstrates that an individual's metabolic profile of TPM could be used to predict the person's cognitive deficit. We note that in some of clinical studies no clear relationship was found between average plasma concentration of topiramate and clinical response such as seizure reduction (Rosenfeld, 1997; Elterman, 1999). Our finding may provide some clinical insights for physicians facing decisions involving the therapeutic management of cognitive side effects of TPM. TPM exposure (plasma drug levels), as a more accurate measure of drug concentration than dose administered, might serve as a reliable predictor of the extent of individual differences in TPM-induced impairments in executive brain function and cognitive behavior.

Behavioral measures such as reaction time contain the contribution of many neurophysiological processes including sensory processing, decision-making, and movement execution. We further examined the physiological basis of TPM's adverse

effects on cognition by using the ERP method. Following the onset of the probe stimulus, ERP differences between TPM and placebo conditions were transformed into Z scores, which take into account the intrinsic variability between the two ERP traces by incorporating the ERP differences during the pre-stimulus period. Topographic activation and temporal (time course) plots of the Z score reveals that significant differences between TPM-related ERP and placebo-related ERP begin to emerge after around 400 ms in the frontal and left temporal area of the brain, suggesting that it is not the sensory processing but the later memory processing stages in frontal and left temporal area that are affected by TPM. Further, this finding may also provide an explanation of TPM's known effects on language production.

Past AED studies (Chung et al., 2002; Ozmenek et al., 2008; Sun et al., 2007) have employed ERP profiles to measure neuro-electrophysiological effects of these drugs. These studies tend to focus on ERP component variations. For example, N160 component augmentation (corresponding to N100 component of the visual ERP occurring between 130 and 180 ms) to match visual stimuli was reduced by phenytoin in healthy young adults compared with placebo (Chung et al., 2002). While according to some reports, the latencies and amplitudes of the P300 component were significantly affected by older AEDs, such as phenobarbital, carbamazepine and valproate (Chen et al., 1996; Enoki et al., 1996), others (Smith et al., 2006) reported that in healthy subjects, P300 at Pz electrode was not significantly affected by TPM, and the main effect is that TPM blocked enhancement of positive-going slow wave that followed the P300. More recently, Jung et al. (2010) found that P200 component was significantly increased at Fz electrode by TPM.

None of the above cited studies provide enough evidence on whether TPM's language related cognitive deficit is related to a unique disruption of language mechanisms or simply reflects a more general disruption of frontal executive functions. The following reasons may explain why some of previous works did not report findings similar to ours: (1) They used small numbers of scalp electrodes for EEG recordings and analyzed only a couple of channels, which makes a whole brain function mapping difficult; as a result target brain regions of the drug could not be identified. (2) Previous studies employed n-back task and analyzed the data collected from the entire task period mixing ongoing memory processed and stimulus processing. We employed a sequentially presented modified Sternberg visual working memory paradigm so that we can see the clear temporal and spatial development of neural activity. (3) For ERP analysis, some averaged ERP over different treatment conditions. This can dilute the effect of unique drug effects on EEG patterns. Our results on post-TPM's temporal and topographical information, to our best knowledge, is the first study that showed possible target brain regions along with temporal information that may account for TPM's related cognitive dysfunction using scalp EEGs. Our interdisciplinary work as a whole leveraged the synergy effect between clinical pharmacology, linguistics, engineering, and neuroscience – disciplines that traditionally do not interact.

Table 4-1. Study timetable

Procedures	Sessions Baseline	1st Drug	2nd Drug	post-Baseline
Medical history/demographics	O			
Vital signs		O	O	
Drug administration		O	O	
Neuropsychology battery	O	O	O	O
WM task w/ EEG recording	O	O	O	
Blood draw		O	O	

Table 4-2. Summary of neuropsychology battery

	Time
Medical College of Georgia (MCG) test	< 15 min
Symbol Digit Modalities Test (SDMT)	90 sec
Controlled Oral Word Association Test (COWAT)	1 min
Category Fluency	1 min
Category Switching	1 min
Action Verb Fluency	1 min
Boston Naming Test (BNT)	< 3 min
Minnesota Picture Description	< 5 min

Table 4-3. Trial rejection rate (%)

	Sessions			
Subject	Baseline	1st Drug	2nd Drug	Average*
1	33.3	24.5	11.7	23.2
2	8.1	14.5	4.5	9.0
4	8.3	14.5	8.3	10.4
5	17.6	11.9	15.5	15.0
6	18.6	17.9	9.5	15.3
7	5.7	18.3	10.0	11.3
8	27.6	19.0	12.1	19.6
9	2.9	7.9	4.3	5.0
10	39.3	22.9	13.3	25.2

* The average trial rejection rate across subjects was 14.9%

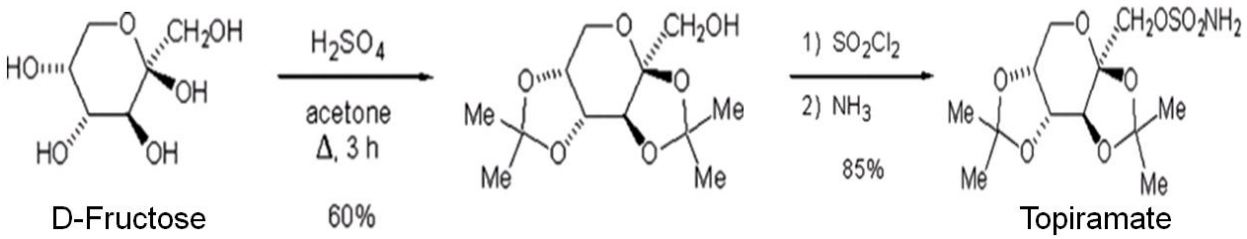

Figure 4-1. Topiramate and its synthesis

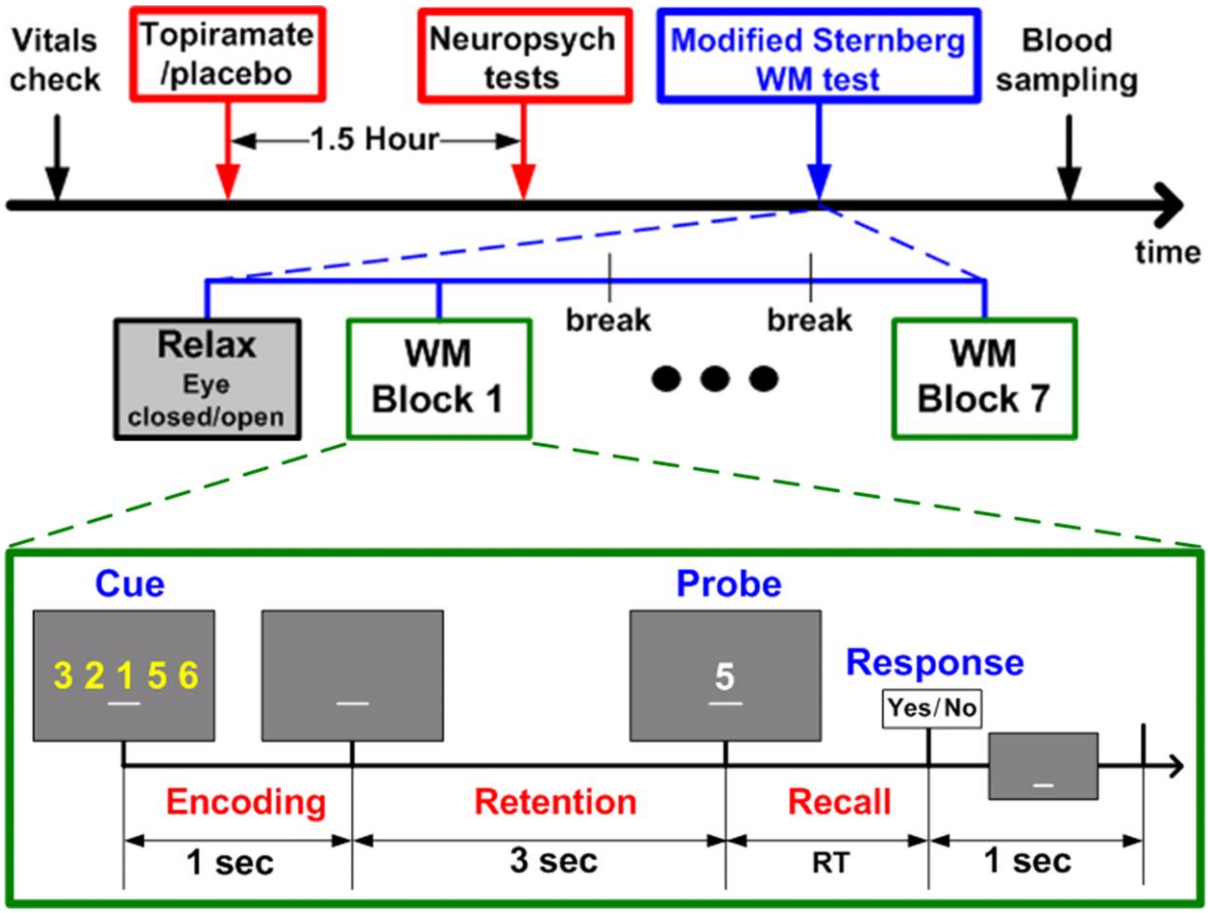

Figure 4-2. Study timeline and working memory paradigm

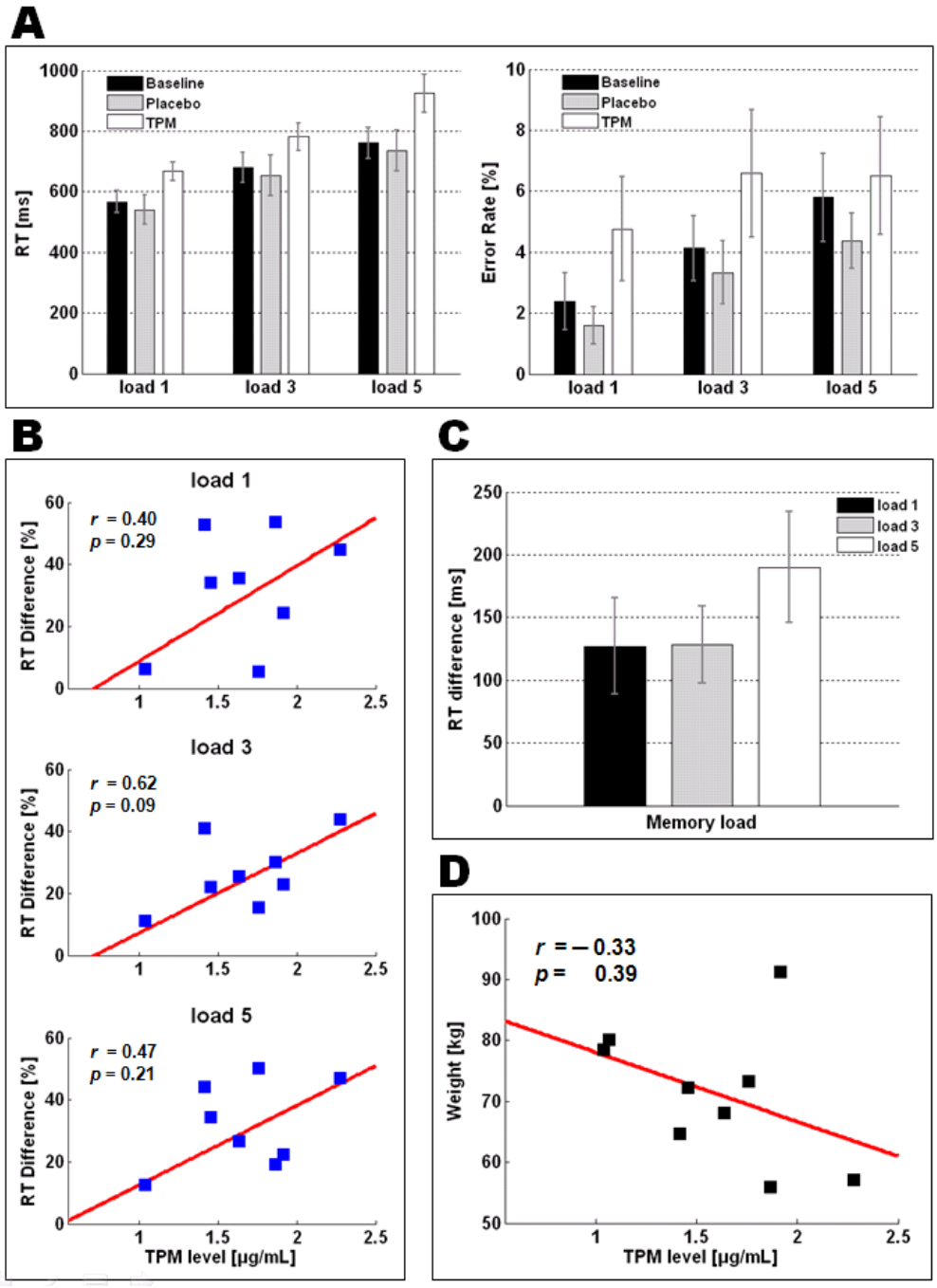

Figure 4-3. Behavioral results and topiramate concentration analysis. A) Subjects' average reaction time (RT) on the left and error rate (right) for each memory load for all three conditions. The standard errors are shown as error bars. B) Correlation between an individual's drug concentration in blood taken at the end of each recording (see Fig. 1) and the percentage RT difference between TPM and placebo sessions. C) Average of sheer RT difference (TPM – placebo) from nine subjects for memory loads. D) Negative correlation between a subject's weight and the drug level in blood. *Spearman's rank correlation coefficient is r = -0.74 (p = 0.04) when an outlier was excluded.

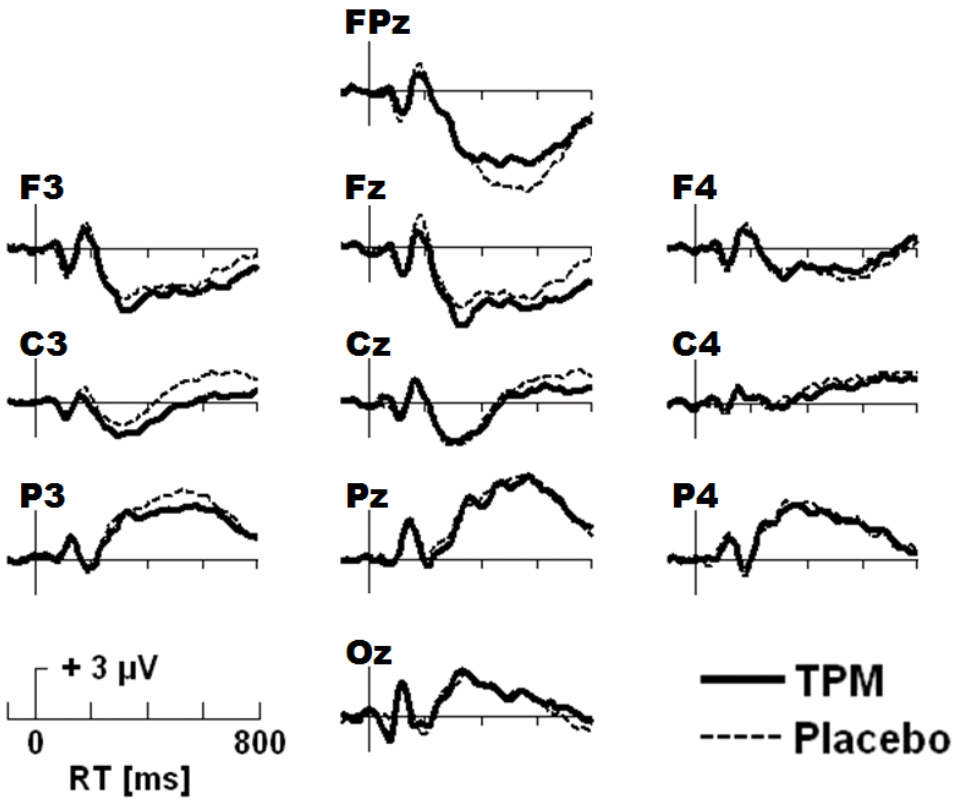

Figure 4-4. Grand averaged ERPs in the TPM (solid line) and in the placebo (dashed line) conditions elicited by onset of the probe digit marked as 0 ms (see Fig. 1) for memory load 5.

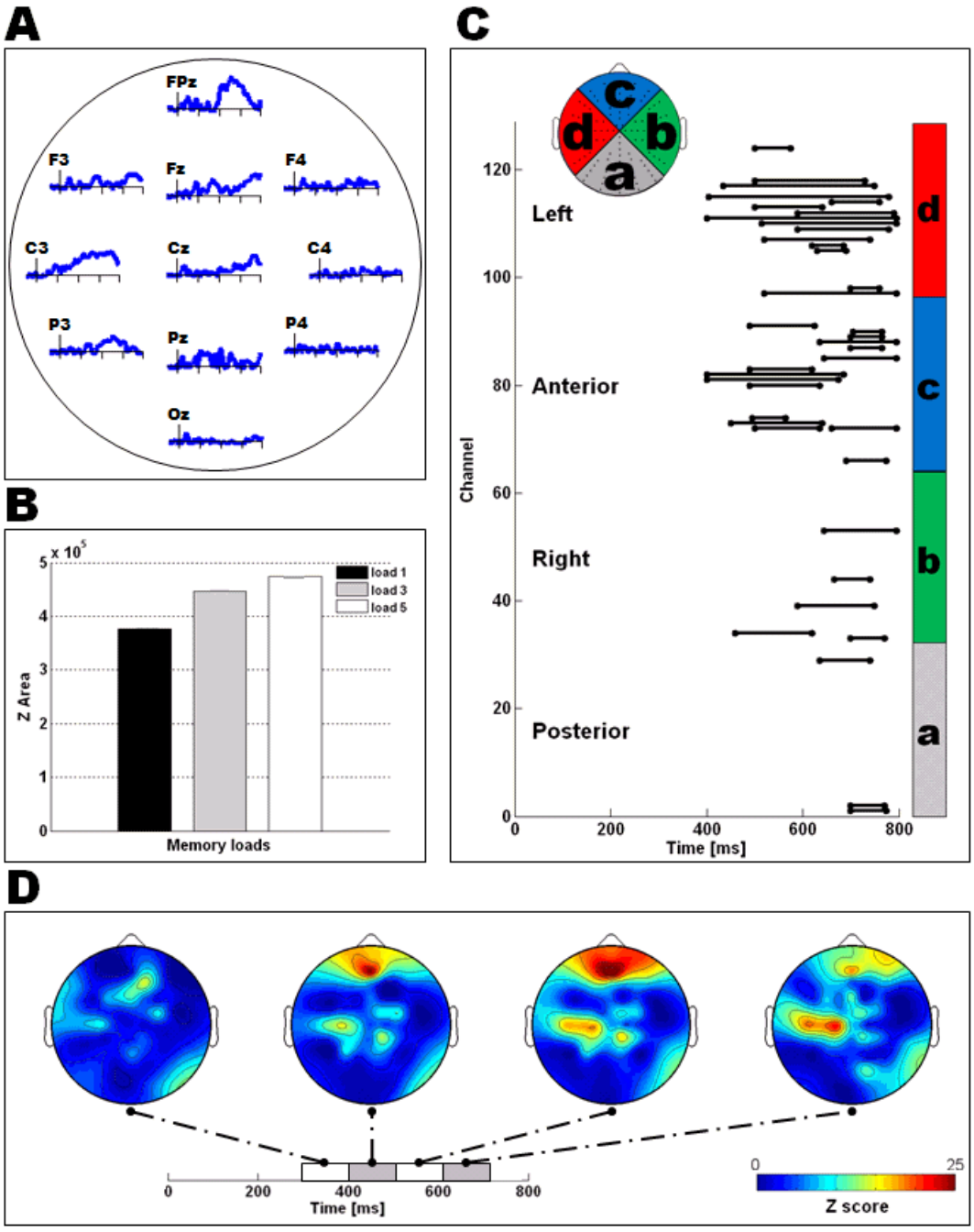

Figure 4-5 Z score based analysis on the differences between the TPM and placebo conditions. A) Time courses of z score computed from grand averaged ERP differences for load 5. B) Defined as sum of the integral of z score function in the interval from 0 to 800 ms for all 128 channels, z areas were compared for different memory loads. C) Temporal information when the effects are significantly different. 128 channels are mapped on into four brain regions: a, b, c and d representing posterior, right side, anterior and left part of a brain respectively. Channels are numbered from 1 to 128 according to BioSemi recording system convention (http://www.biosemi.com/). D) Topographic z score amplitude map averaged over time blocks of 100 ms showing where the difference is significantly larger.

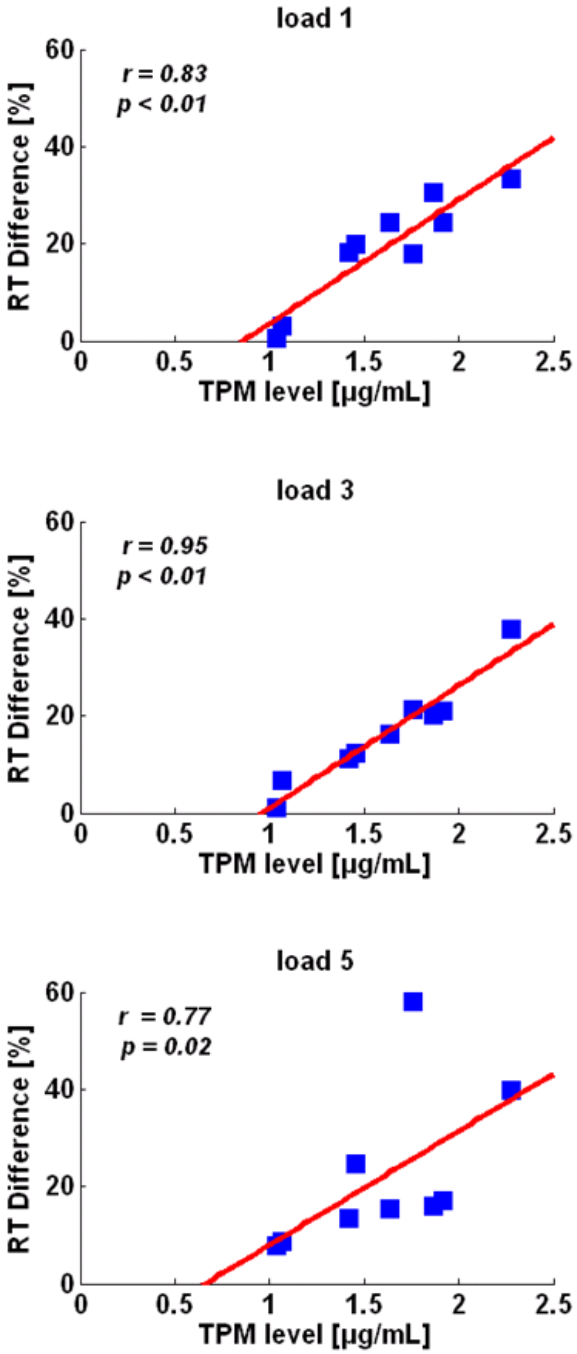

Figure 4-6. TPM vs. baseline comparison I. TPM plasma level correlation with percentage RT differences by Spearman's rank correlation coefficient (SRCC). *without outlier (subject #7*) r=0.86, p=0.01* for load 5.

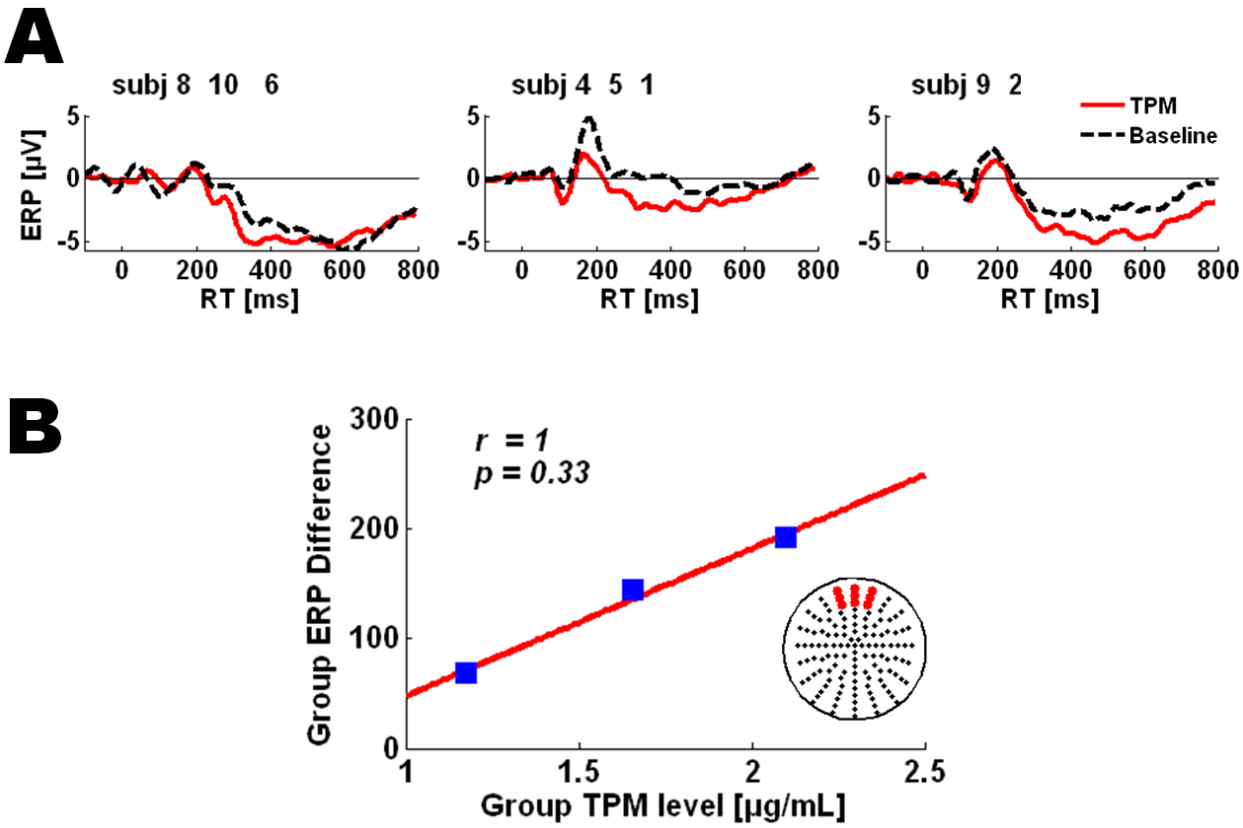

Figure 4-7. TPM vs. baseline comparison II. A) ERP traces from the nine frontal channels. Subjects are sorted and grouped into three according to their TPM- and baseline-related ERP difference magnitudes: small (subjects # 8,10,6), medium(subjects #4,5,1) and large(subjects # 9 2) group. B) The group ERP difference and corresponding group TPM serum level correlation.*An outlier is excluded from the analysis.

CHAPTER 5
EFFECTS OF TOPIRAMATE ON ONGOING EEG ACTIVITY

Backgrounds

Topiramate [2,3:4,5-bis-O-(1-methylethylidene)-β-D-fructopyranose sulfamate] is a long-acting and relatively nontoxic antiepileptic drug (Shank et al., 1994) available worldwide. A number of studies have been conducted to examine the anticonvulsant mechanism of action of TPM, such as: (1) activity-dependent attenuation of voltage-dependent sodium currents, possibly by stabilizing sodium channels in their inactivated state (Zona et al., 1997; Taverna et al., 1999); (2) inhibition of AMPA/Kainate receptors (Gibbs et al., 2000); and (3) inhibition of the carbonic anhydrase (CA) enzyme, particularly isozymes II and IV (A1). And more recently, a new mechanism is proposed: inhibition of depolarizing GABAA mediated responses (Herrero et al.,2002). Nonetheless, its mechanism of action has yet to be clearly elucidated and very few of them tried to explain the mechanisms in terms of encephalopathic EEG connectivity patterns. In chapter 3, we observed that ongoing activity during the retention period of the working memory task was modulated by memory load. In chapter 4, we looked at how behavioral performance and ERPs were affected by TPM in the same experimental task. In the current chapter, how TPM is modulating ongoing brain activity, particularly the retention period of the working memory task, is examined. Specifically, we first looked at the resting state (with eye closed) where subjects were not involved in any mental task, making the period a simple, no confounding-factor state. Then, power and coherence modulations by memory load for all test conditions were analyzed. We also looked at the relation between drug concentration and power modulation in different brain regions and compared the results with previous studies (Coulter et al., 1993;

White et al., 1997; Gibbs et al., 2000). We note that, in contrast to previous studies where only a few electrodes were used (Smith et al., 2006; Salinsky, 2002; Meador, 2001), in our study EEG signals from all 128 channels were utilized. In addition, the power difference between placebo and TPM was used to correlate with drug concentration. Our results shed some light on the possible TPM mechanisms affecting ongoing EEG activity.

Materials and Methods

Subjects

Nine subjects (mean age 22 ± 2 years, 7 males, 2 females, all right-handed) out of eleven volunteers whose data were used in chap 4 were selected for this chapter. They all reported normal neurological and psychiatric conditions with normal or corrected-to-normal vision gave written informed consent and participated in the study. Two subjects were excluded: one was suspected of drug abuse and the other did not finish all the recording sessions.

EEG Recording

The electroencephalogram (EEG) recording was conducted in the chamber (ETS-Lindgren, Illinois) described in Chapters 3 and 4. A 128-channel BioSemi ActiveTwo System was used for scalp EEG recording at a sampling rate of 1024 Hz. For eye movement monitoring, six additional flat-type electrodes were used: (a) two on each lateral side of both eyes to monitor horizontal electroculogram (hEOG), (b) two above and below the left eye to monitor vertical eye movement (vEOG), and (c) two on the left and right sides of preauricular points. The modified Sternberg's working memory paradigm was delivered by a custom program written in BeriSoft Experimental Run-Time System (ERTS) language, and the key press response was registered by an

EXKEY microprocessor logic pad (http://www.berisoft.com) to sort out correct trials in an offline analysis.

Data Preprocessing

Data analysis was performed using BESA 5.2 (www.besa.de) and custom functions written in MATLAB 7.5 (www.mathworks.com). The raw data were band-pass filtered from 1 to 55 Hz and downsampled to 200 Hz. Only trials with correct responses were considered for further analysis. Trials with any of the following factors were excluded as in Chapter 4: (1) EOG exceeding 120 μV, (2) excessive muscle or movement artifacts, and (3) extreme response times (> 2.0 s or < 0.10 s). The remaining artifact free data were re-referenced against the average reference (Nunez et al., 1997; Ferree, 2006). For the task conditions the last two seconds of the retention period were selected for analysis.

Spectral Power and Coherence Estimation

The MultiVariate AutoRegressive (MVAR) time series modeling method was used to estimate power spectra (Ding et al., 2000). For alpha frequency band percentage change analysis, power spectral densities (PSDs) were averaged over 8 to 13 Hz range then averaged across subjects for each channel. Percentage change between two different conditions (either two different treatment sessions for the same memory load or different memory loads for the same treatment) is defined by the following formula:

$$\frac{final - initial}{initial} \times 100$$

Channels in Regions of Interest (ROI) were selected where we can observe prominent changes (common channels when it comes to two different treatments comparison). But for frontal lobe, nine channels were selected as shown in Figure 5-2.

The values from the selected channels were averaged and then averaged again across subjects. Coherence analysis follows the same procedure as in power estimation.

Significance Test

To provide statistical significance, relative power data (Figure 5-3) obtained from two treatment sessions were tested using one-way ANOVA with a factor: drug treatment with two levels (TPM and placebo). In the coherence analysis, one-way ANOVA or paired t-test were applied depending on the nature of the comparison (Figure 5-5B and C respectively). The factor is memory load with three levels (load 1, 3 and 5) for the ANOVA test. For each subject, coherence values were averaged over the alpha range for each treatment before the paired t-test.

Results

Resting State Power Analysis

Prominent spectral peaks in the alpha band (8 to 13 Hz) are seen for both TPM and placebo conditions. Our analysis mainly focus on this frequency band. As shown in Figure 5-1, resting state (eye closed) percentage alpha power changes (TPM vs. placebo) were calculated using the MVAR method. The strongest alpha increase is seen over the occipital-parietal areas. Power modulations for some channels including Pz and other parietal channels are over 100 %.

Alpha Power Modulation by TPM during Working Memory Retention

Now we examine the modulation of alpha power by TPM during working memory retention. Relative alpha power change in TPM session against placebo for memory load 5 was calculated and topographically presented in Figure 5-2A. The magnitude of power changes during this period across all channel locations is less than 35 % which is in agreement with previous studies (Busch et al., 2003; Enoch et al., 2002; Klimesch,

1996; Klimesch et al., 2007; Placidi et al., 2004; Ray et al., 1985; Salinsky et al., 2002; Salinsky et al., 2004; Salinsky et al., 2007). Higher alpha modulation in posterior and mid frontal region and mild change in prefrontal region were observed. Enhanced posterior alpha in the topography showed an interesting pattern: contours of occipital lobes including longitudinal cerebral fissure. The degree of modulation is proportional to the TPM concentration level when alpha power from posterior channels (Figure 5-2C) and the TPM level were correlated (*r=0.81, p=0.02* by Spearman method) as shown in Figure 5-2B.

Power and Coherence Modulation by Memory Load

In Chapter 3 we showed that alpha power in visual cortex and frontal-visual coherence in the alpha band increase as a function of memory load. Here we investigate whether the same phenomena holds for the placebo condition and for the TPM condition. The results are shown in Figure 5-3. There was a trend throughout all conditions for power spectra: the higher the memory load, the higher the visual alpha. A one-way ANOVA found that alpha power was affected by memory load for baseline ($F_{2,24}$ = 4.93, p = .016) and TPM ($F_{2,24}$ = 3.67, p = .041) conditions. Tukey-Kramer HSD pair-wise comparisons indicated that there was significant difference between load 1 and 5 for both treatments (p < .01 for baseline and p = .046 for TPM). For the placebo condition, no statistical differences were found although the general trend was observed. For frontal-visual coherence, a similar pattern of coherence increase with memory load was observed as in power spectra for baseline and placebo conditions, but the memory load effect was opposite for the TPM session: the higher the memory load, the lower the alpha coherence. There was significant difference between load 1

and 5 (p = .038) for baseline and between load 3 and 5 (p = .048) for TPM but no significance was found for the placebo session.

Visual Alpha Modulation

Alpha power modulations by memory load in visual area were compared for TPM and placebo sessions in Figure 5-4. Average alpha power change between load 5 and load 3 was significantly higher in visual area (red dots in the topography plot) for TPM condition (p < .01). Visual channels where large alpha modulation was observed for both conditions were selected for analysis.

Alpha Modulation and Drug Concentration

For the TPM session, alpha power modulations were computed for load 3 and 5. As shown in Figure 5-5B, frontal area alpha power change shows stronger correlation with drug concentration level than that of visual area (*r=0.81, p=0.01 and r=0.48, p=0.19* for frontal and visual area respectively, by the Spearman method). Here individuals blood sample were collected at the end of recordings and were analyzed at the University of Minnesota**.**

Discussion

In this chapter we examined how TPM modulated ongoing brain activity, particularly alpha oscillations, during rest and during working memory maintenance. During rest TPM generally increased alpha power in the posterior areas. Given that posterior alpha is involved in functional inhibition, this finding is consistent with one of TPM's mechanisms of action: inhibition of depolarizing GABAA mediated responses (Herrero et al., 2002). Several studies have reported on the TPM's effect on GDPSPs or GABAA receptor-mediated depolarizing postsynaptic potentials (Kaila et al.,1997; Herrero et al.,2002): (1) GABAA-induced depolarization participates in the generation of

ictal discharges (Higashima et al., 1996; Lopantsev and Avoli, 1998; Perez Velazquez and Carlen, 1999; Kohling et al., 2000); (2) other CA inhibitors have anticonvulsant properties (Resor et al., 1995); and (3) the concentration of TPM that reduces GDPSP is within the therapeutically relevant range (Shank et al., 2000; Dodgson et al., 2000). The same anticonvulsant properties of TPM might underlie the observed alpha power increase in occipital-parietal lobes.

After establishing that TPM can affect alpha activity we further examined the functional correlates of alpha during working memory retention under the influence of TPM. For all test conditions (baseline, placebo, TPM) we observed the classical alpha power modulation pattern by working memory load: the higher the load, the higher the alpha power. At memory load 5, TPM enhanced posterior and some mid frontal regions of alpha power when compared to the placebo session, and the degree of the alpha modulation is proportional to the TPM blood concentration level: higher the TPM concentration, the higher the frontal and posterior alpha modulation. Interestingly, the topographical map of the correlation coefficient posterior regions revealed a pattern that resembles the contour of the occipital lobe including the longitudinal cerebral fissure.

Next we considered the effect of TPM on frontal-visual coherence in the alpha band. For baseline and placebo conditions, the frontal-visual coherence showed similar patterns. For the TPM condition, a reverse pattern was observed, suggesting that TPM may disrupt long distance communications between frontal and posterior area. It is known that TPM inhibits the carbonic anhydrase (CA) enzyme, particularly isozymes II and IV (Kida et al, 2006). In addition, TPM, as a sulfamate-substituted monosaccharide, is also a weak inhibitor of carbonic anhydrase (Enoch et al., 2002; Gardocki et al.,

1986). Although the function of CA is not well understood, a certain type of CA isoenzymes (CA II) have heavy human brain concentrations in oligodendrocytes and myelin (Kida et al., 2006). Oligodendrocytes are essential for the formation of myelin sheaths in the CNS, which also promote neuronal survival, increase axonal stability and induce local accumulation and phophorylation of neurofilaments within the axons (Colello et al., 1994; Sanchez et al., 2000; Wilkins et al., 2003). Based on these ideas, it has been suggested that one of TPM's mechanisms for cognitive impairments may be related to white matter dysfunction affecting neuronal connectivity (David Loring, private communication) although it is not clear how long until this effect will take place. In addition to the effect on executive functions such as working memory, TPM is also known to affect language production (Ojemann et al., 1999). It is reasonable to speculate that the language deficits induced by TPM could be attributable to network disruption although no studies to date have examined this issue.

Although recent AED studies have combined EEG recordings and psychometric tasks to measure both behavior and fast changing neural activities, these studies tend to use small numbers of recording channels (Veauthier et al., 2009; Park et al., 2009; Loring et al., 2007; Meador et al., 2007; Placidi et al., 2004), which makes brain function mapping difficult. In addition, some of the tasks used make it difficult to clearly separate ongoing activity periods from stimulus processing periods, negatively impacting the interpretation of data. This may explain why some of the previous studies did not report findings similar to what we found here. For example, one of our key results is that percentage alpha power increase with TPM, when compared with the placebo condition, is proportional to TPM blood concentration. A previous study on TPM and working

memory did not find such an effect. Upon further examination it is clear that these authors used a n-back task and analyzed the data collected from the entire task period mixing ongoing memory process and stimulus processing. We employed a modified Sternberg working memory paradigm where subjects see the digit cues all at once rather than sequentially. The main advantage of this paradigm over the classical Sternberg task is that the periods of encoding, retention and recall are all well separated in time so that it allows us to study both the temporal and spatial development of neural activity during the different stages of working memory process. This enables us to see clear alpha modulation during ongoing periods (Marciani et al., 1999; Placidi et al., 2004; Meador et al., 2005).

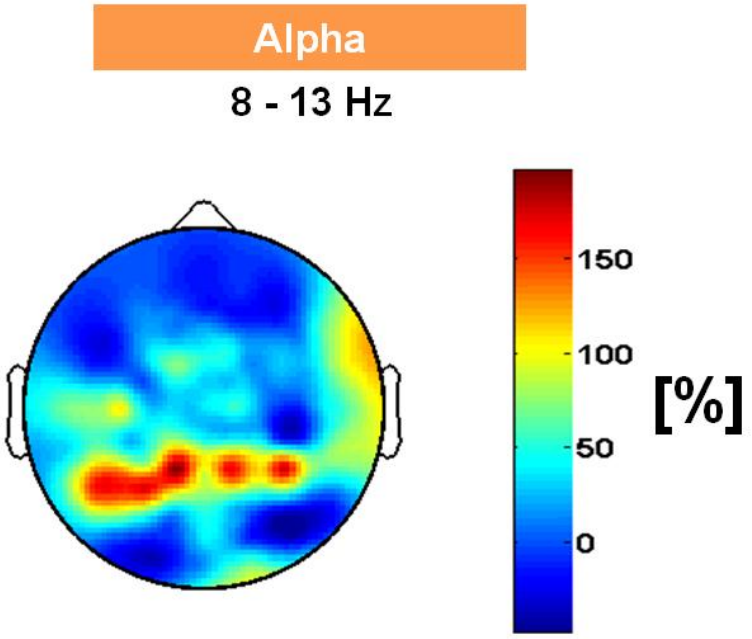

Figure 5-1. Percentage power change (TPM vs placebo) in alpha (8–13 Hz) frequency ranges during the eye closed period.

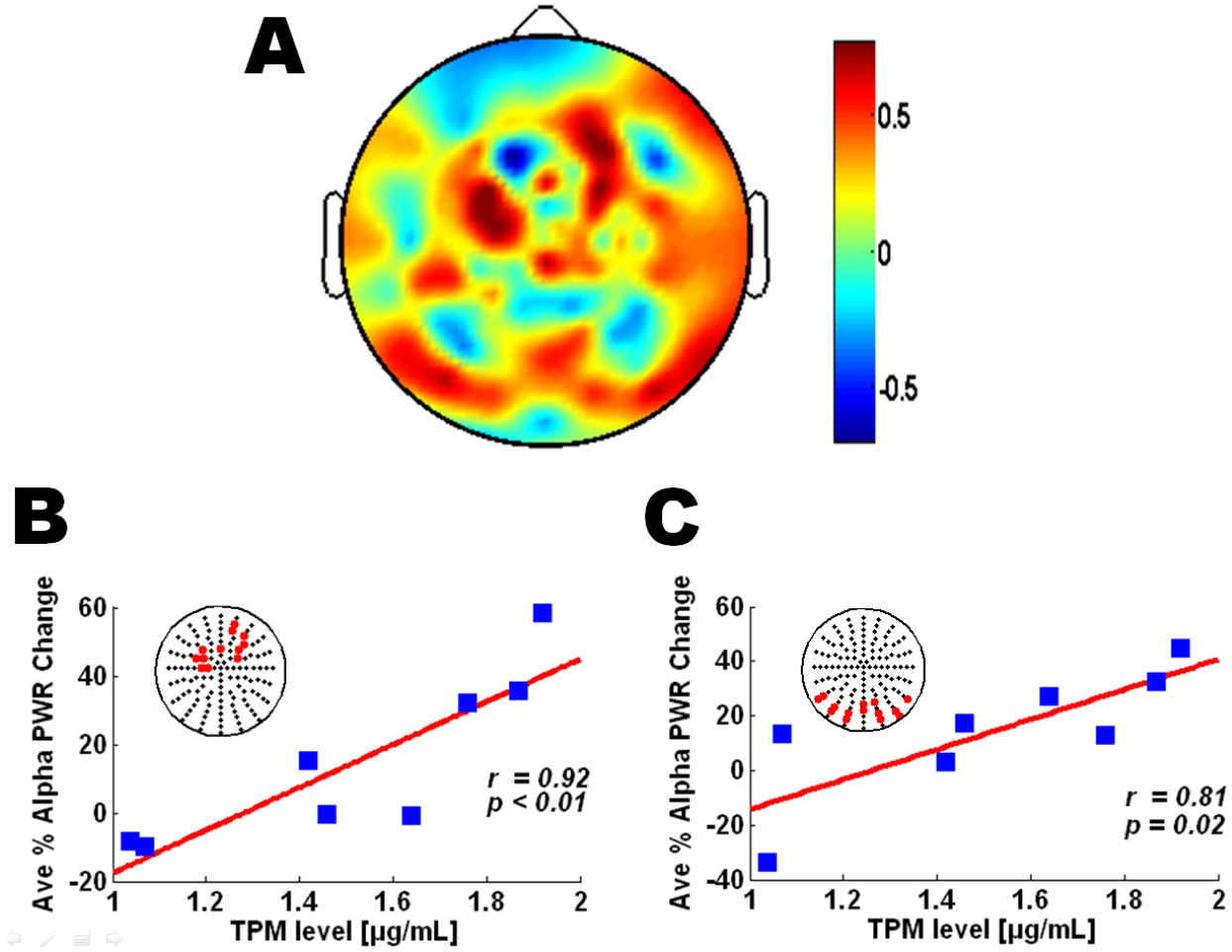

Figure 5-2. Alpha power modulation. A) Topography showing regions of increased alpha power when TPM and placebo sessions are compared for load 5. B) Correlation between alpha power change and drug concentration level. Selected channel locations for the correlation analysis were shown in the plots.

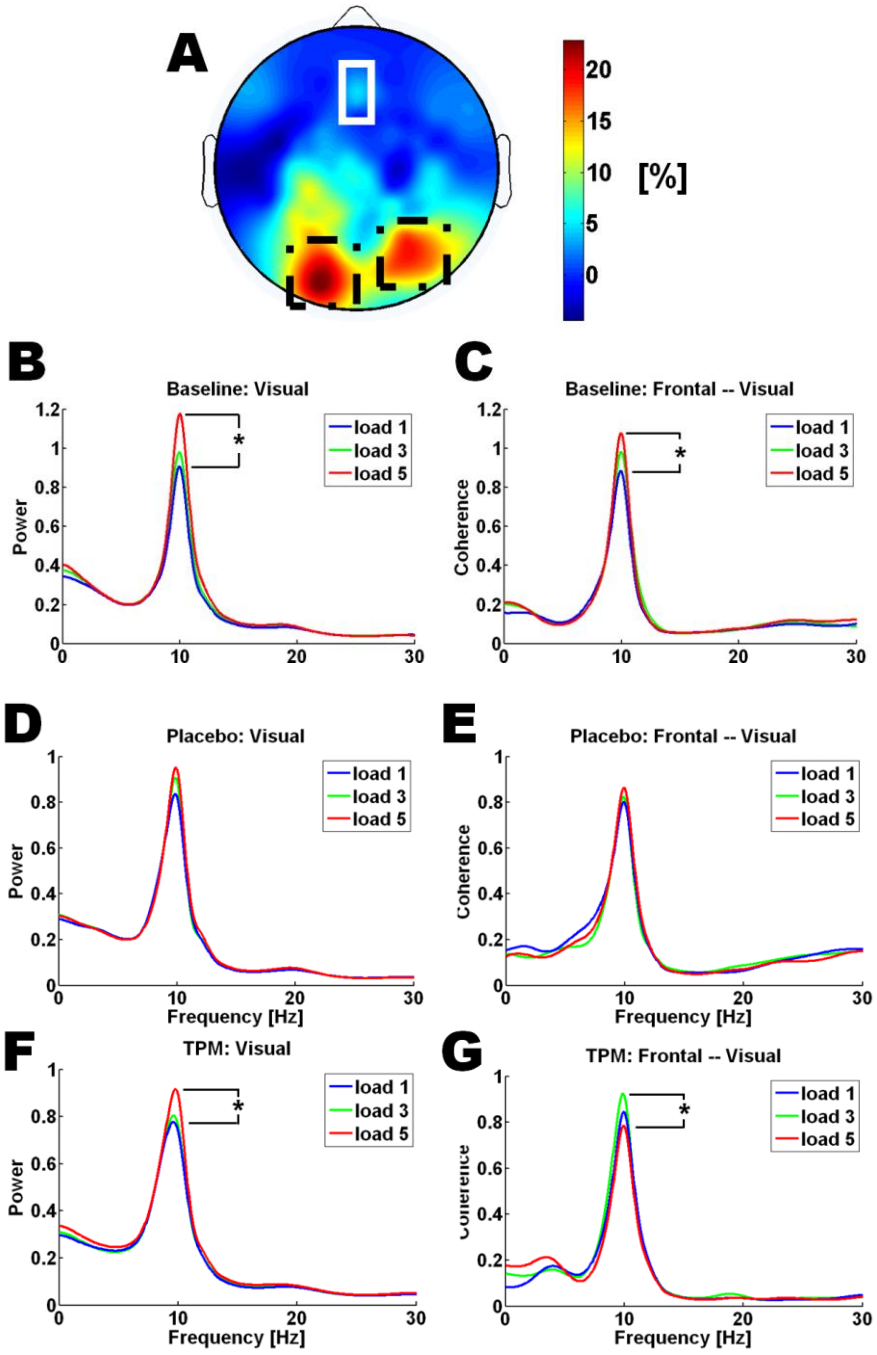

Figure 5-3. Memory load modulations of power and coherence for baseline (B, C), placebo (D, E) and TPM (F,G) sessions. Power modulation by memory load for TPM. Alpha Power spectra for each memory load were calculated in visual regions (black dashed box). Coherences were calculated between the midline frontal channels (white solid box) and posterior visual channels. One-way ANOVA test were done followed by the Tukey-Kramer HSD method for post-hoc analysis when there is a significant difference (asterisk indicated a significant difference between conditions). * significance at the of 0.05 by one-way ANOVA and Tukey-Kramer HSD.

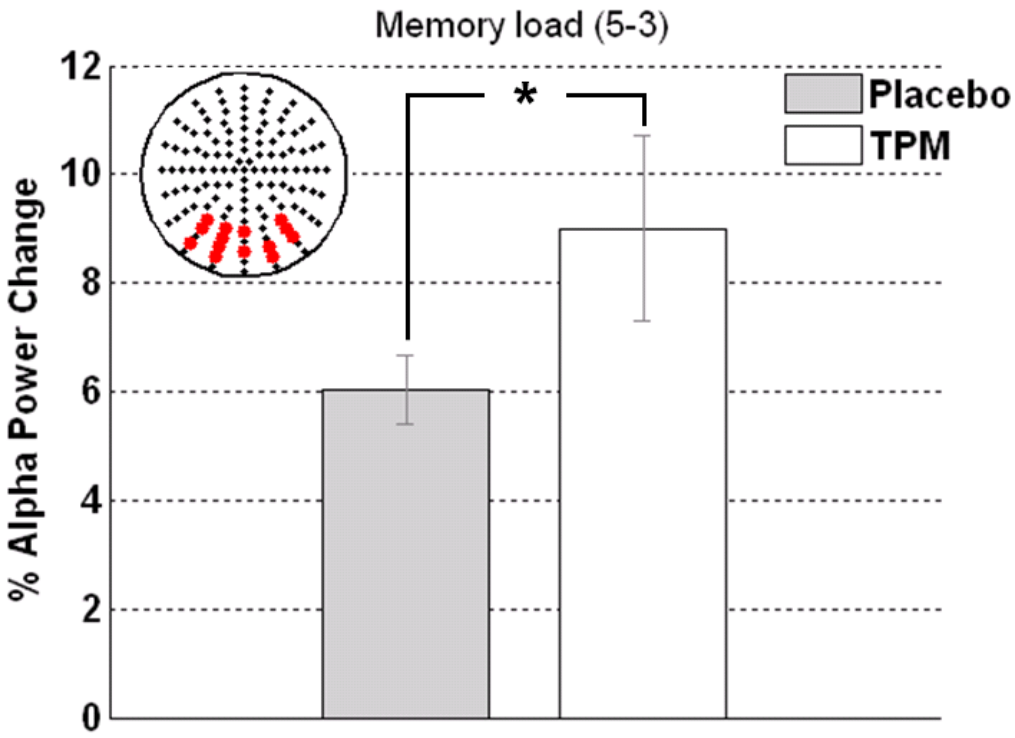

* $p < 0.01$ at significant level of 0.05 by paired t-test

Figure 5-4. Visual alpha power modulation comparison between TPM and placebo conditions during memory retention period. In visual regions, average alpha power change by memory load (from load 3 to load 5) for TPM condition was larger than that of placebo. Common channels were used for analysis where large alpha power modulations were observed for the conditions.

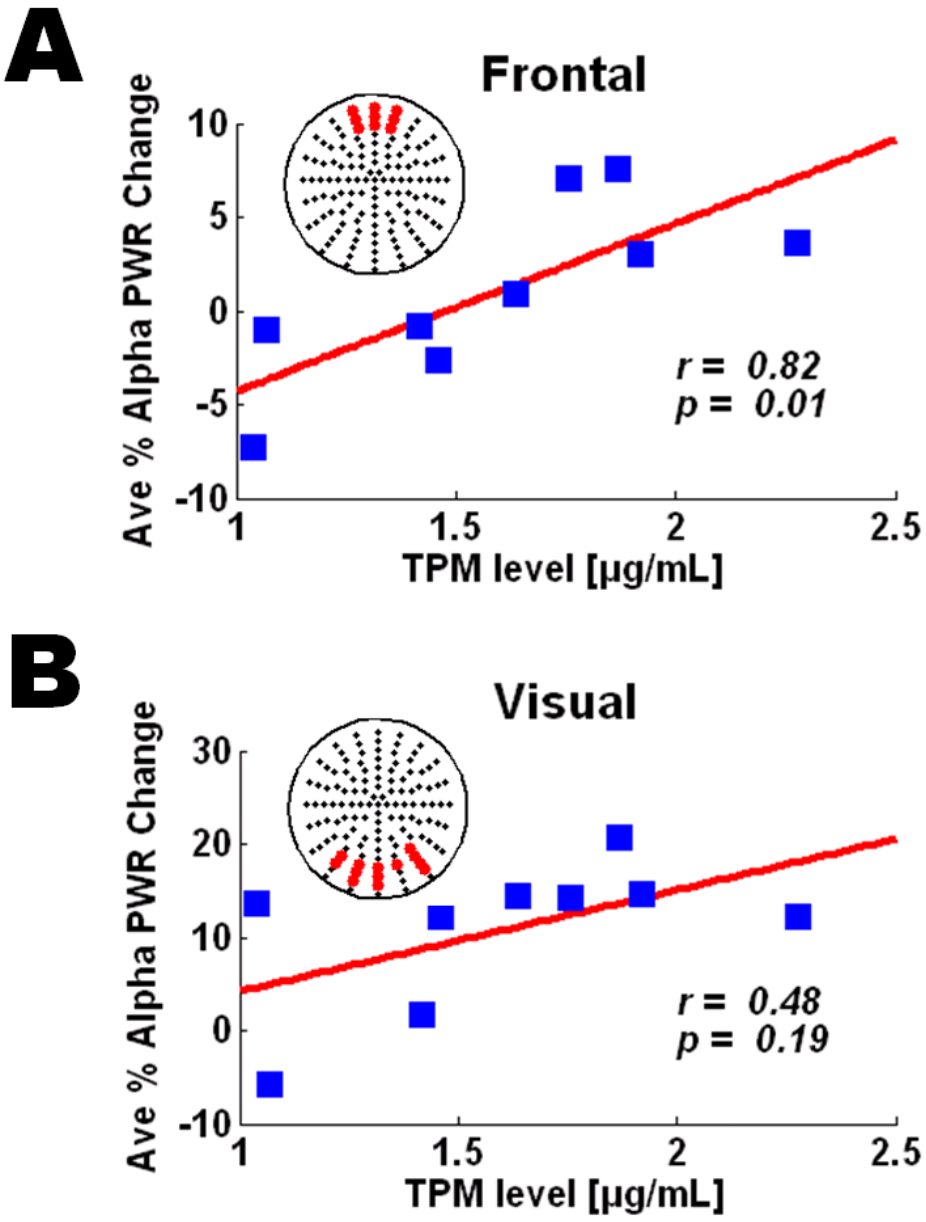

Figure 5-5 Correlation between alpha modulation and TPM concentration in two different regions: frontal (B) and visual area (D) by memory load change (from load 3 to load 5). Correlation in frontal region (A) is stronger than in visual area (C).

CHAPTER 6
CONCLUSIONS

In this dissertation we considered how brain activity is modulated by working memory and by antiepileptic drug topiramate. In the first study, discussed in Chapter 3, we examined behavioral effects and brain oscillations in the scalp EEG of 10 healthy subjects performing a modified Sternberg task where a cue signal containing a set of digits is presented all at once. The memory load is controlled by the size of the digit set which is 1, 3, and 5 in our study. We verified the key behavioral findings of the Sternberg paradigm in that the reaction time is an increasing function of memory load (48 ms/digit). Our results further suggested that the human memory scanning may be a serial and exhaustive process which is in agreement with the original Sternberg observation. In ERP analysis we observed the FN400 component and its systematic increase as a function of memory load in frontal regions. No significant differences in early cortical processing of the incoming stimuli are observed. ERP separation between different memory conditions appears to be the earliest in the frontal areas and become progressively later as one moves toward the middle part of the brain, suggesting that memory processing initiates in the frontal executive areas. Interestingly, another similar latency progression pattern is observed starting in the middle part of the brain and moving toward the visual areas. Multivariate spectral analysis applied to the data during the retention period showed a typical monotonic alpha power increase in visual areas. We also observe increased alpha band Granger causality from frontal to occipital regions for higher memory load and interpret the finding as suggesting a possible top-down inhibition mechanism whereby increased top-down excitatory drive on local inter-neurons in visual cortex leads to decreased cortical excitability and increased functional

inhibition to protect the working memory maintained online. We believe that the study of this chapter provides a better understanding of the working memory modulation of visual alpha oscillations and provide further evidence that this increased oscillations reflected an inhibited visual cortex to protect working memory from interference.

In the second study, discussed in Chapter 4, we examined behavioral and neurophysiological effects of Topiramate (TPM) using the same modified Sternberg working memory test. We observed prolonged RTs for higher memory load in the TPM session which is similar to what we observed in Chapter 3. For the same memory load, however, the RT is increased and the accuracy significantly decreased by TPM, demonstrating the adverse effects of the drug on human cognition. The dependence of behavioral measures and brain responses on the serum levels of TPM were analyzed along with the body weight correlation. We found that (1) a negative correlation exists between the TPM concentration level and the body weight which supports the idea that topiramate distribution appears to be primarily to body water and (2) a positive correlation exists between the TPM level and behavioral performance (percentage RT differences between the drug and placebo/baseline conditions). In other words, the higher the serum concentration of TPM, the larger the ERP difference. This finding supports a previous study showing that the mean topiramate concentrations in patients with impaired CNS functions were significantly higher than those in patients without side effects. We further examined the physiological basis of TPM's adverse effects on cognition by using the ERP method. By contrasting the TPM data with the placebo data we found that the early sensory processing is minimally impacted by the drug but the later memory processing stages in frontal and left temporal areas are significantly

affected by TPM. Further, this finding may also provide an explanation of TPM's known effects on linguistic behavior.

In the third study, discussed in Chapter 5, we examined how TPM modulated ongoing brain activity during rest and during working memory maintenance. We found that alpha power is increased in visual areas during rest under the influence of TPM. As one of TPM's main mechanisms of action is inhibition of depolarizing GABAA mediated responses, this further demonstrates that alpha increase in visual cortex reflects increased inhibition, a conclusion we reached in Chapter 3 using behavioral means and Granger causality. Then we further examined the functional correlates of alpha during working memory retention during the TPM session. We observed the classical alpha power modulation pattern by working memory load: the higher the load, the higher the alpha power, suggesting that alpha oscillations can still be modulated by higher order executive processes despite the influence exerted on alpha by TPM. We also found that, for memory load 5, TPM enhanced alpha power in posterior and some mid frontal regions when compared to the placebo session. Importantly, the degree of alpha modulation by TPM is proportional to the TPM blood concentration level. Interestingly, the topographical map of the correlation coefficient in posterior regions revealed a pattern that resembles the contour of the occipital lobe including the longitudinal cerebral fissure. Next we considered the effect of TPM on frontal-visual coherence in the alpha band. For the TPM condition, the frontal-visual coherence showed reverse patterns from the baseline and placebo sessions: lower coherence value for the higher memory load suggesting that TPM may disrupt long distance communications between frontal and posterior areas. This also can suggest that one of TPM's mechanisms for

cognitive impairments may be related to white matter disruption affecting neuronal connectivity even though it is not clear how long it takes for this effect to occur. Lastly, although visual area was strongly modulated by TPM the frontal areas are more sensitive to the drug concentration.

In summary, in this dissertation, two separate experiments were performed which utilized the same modified Sternberg working memory paradigm in which the digit set to be remember was presented as a single cue stimulus rather than sequentially. This feature has the advantage that the periods of encoding, retention and recall are all well separated in time so that it allows us to study both the temporal and spatial development of neural activity during the different stages of working memory process. For both experiments we collected scalp EEG data from 128 channels from the whole brain and employed both ERP and spectral analysis methods. In the first experiment we gave further physiological meaning to the alpha oscillation and its modulation by working memory load. The second experiment, representing interdisciplinary work leveraging the synergy effect between disciplines that traditionally do not interact: clinical pharmacology, linguistics, engineering, and neuroscience, made contributions to our understanding of how CNS drugs can impact cognition. However, owing to the fact we have no titration period and the drug was given in an acute fashion, our result on TPM here must generally be interpreted with caution when it comes to clinical practice and require further confirmation studies that use a sufficient titration period and eventually use actual epilepsy patients.

APPENDIX A
STERNBERG WORKING MEMORY SIMULATOR

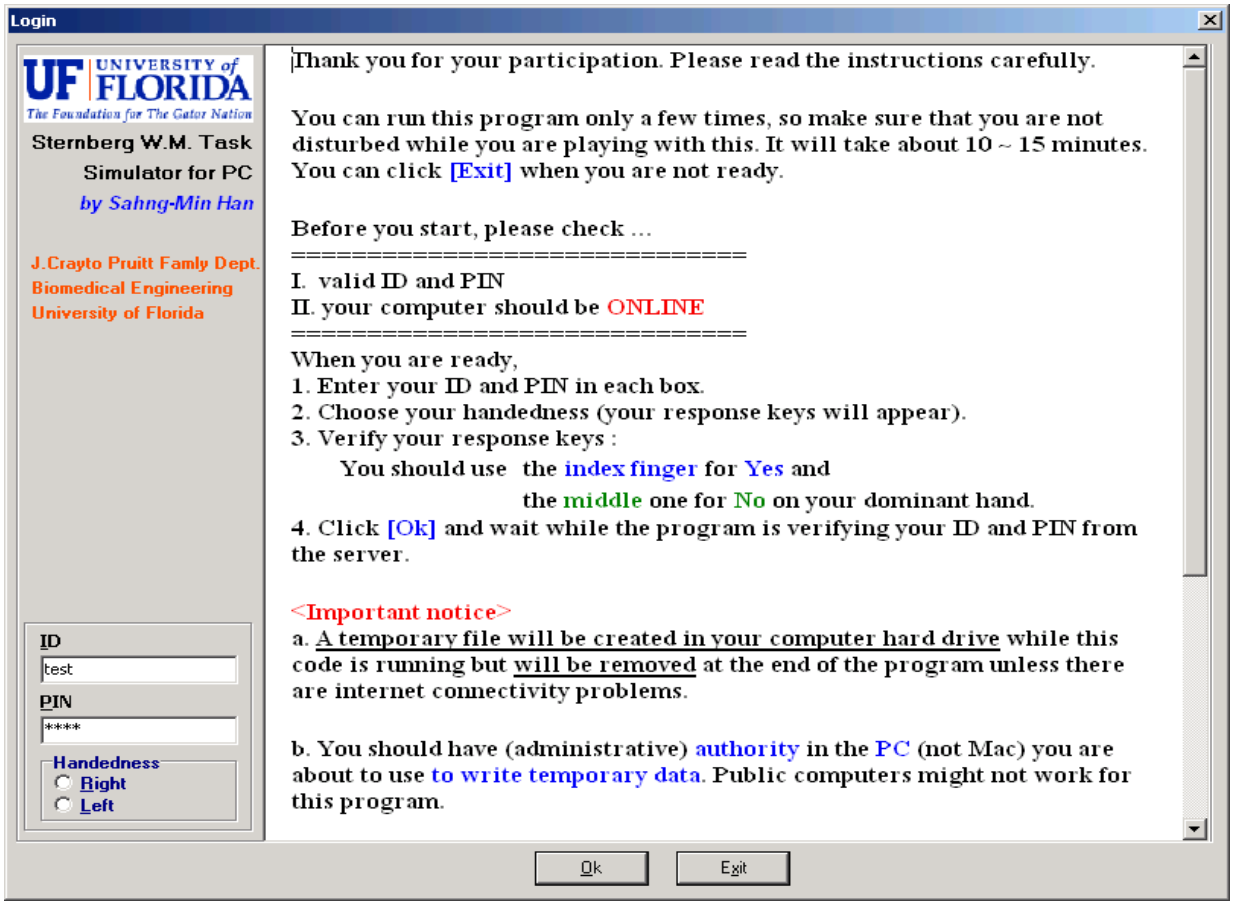

Figure A-1. Log on page

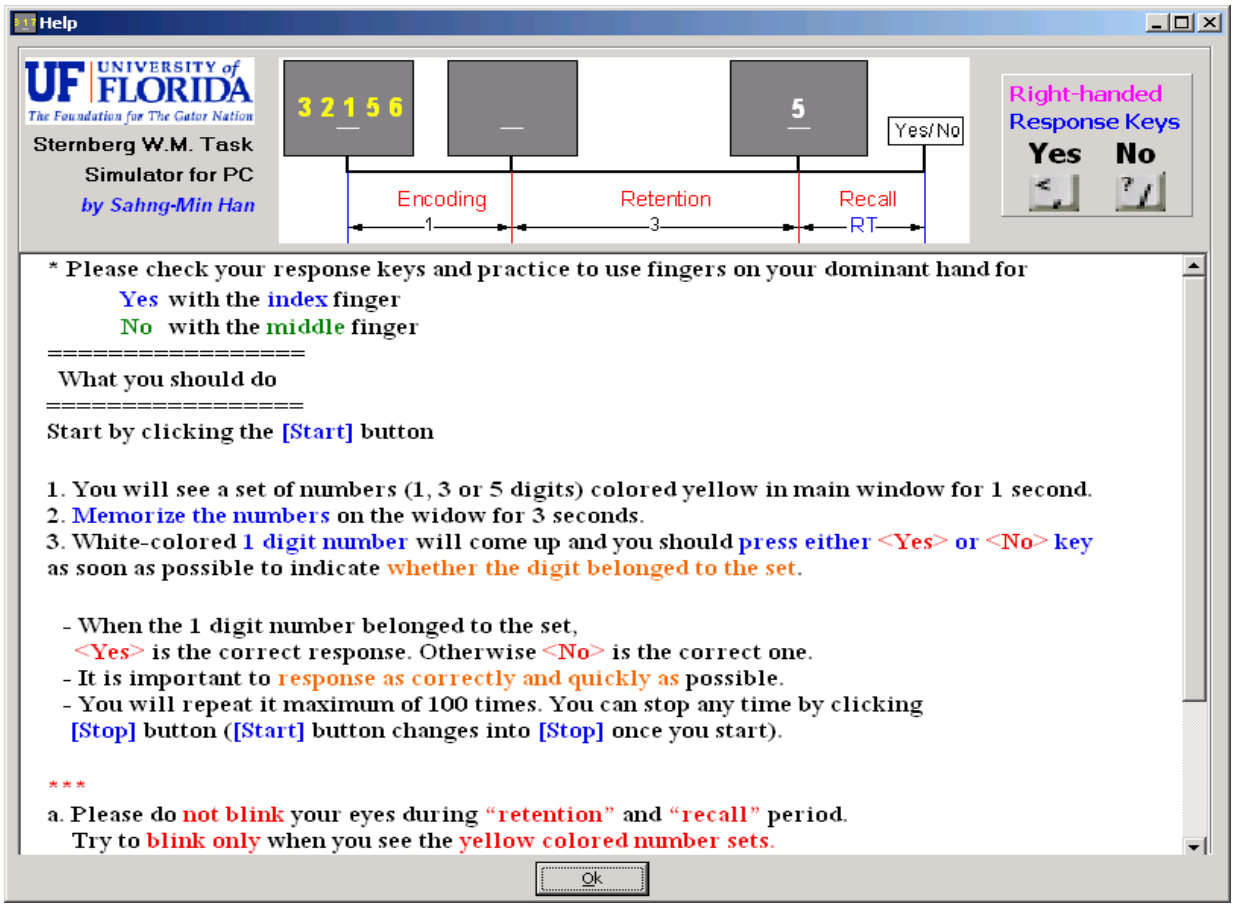

Figure A-2. Introduction page

.

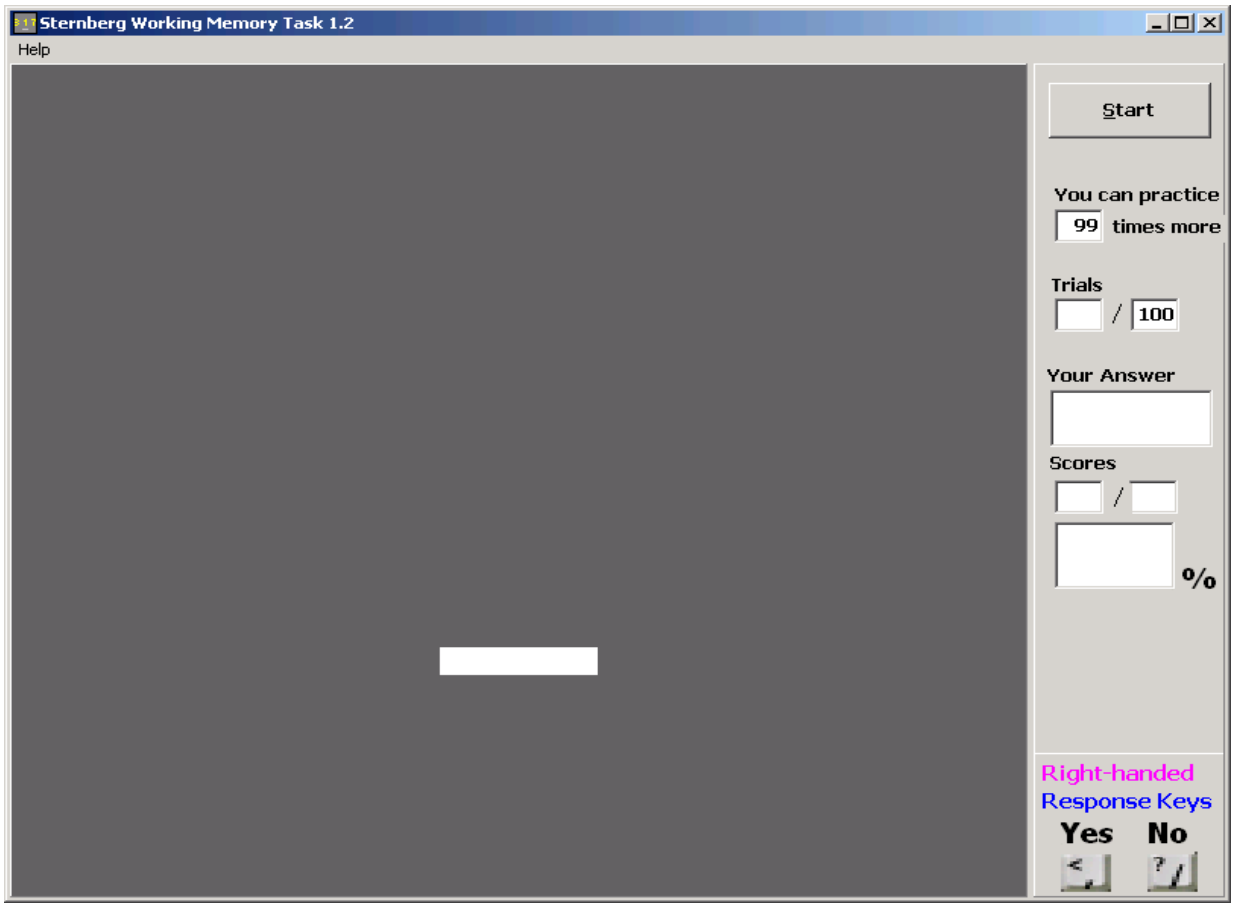

Figure A-3. Actual practice mode

APPENDIX B
MINNESOTA ADAPTIVE PICTURE DESCRIPTION STIMULUS

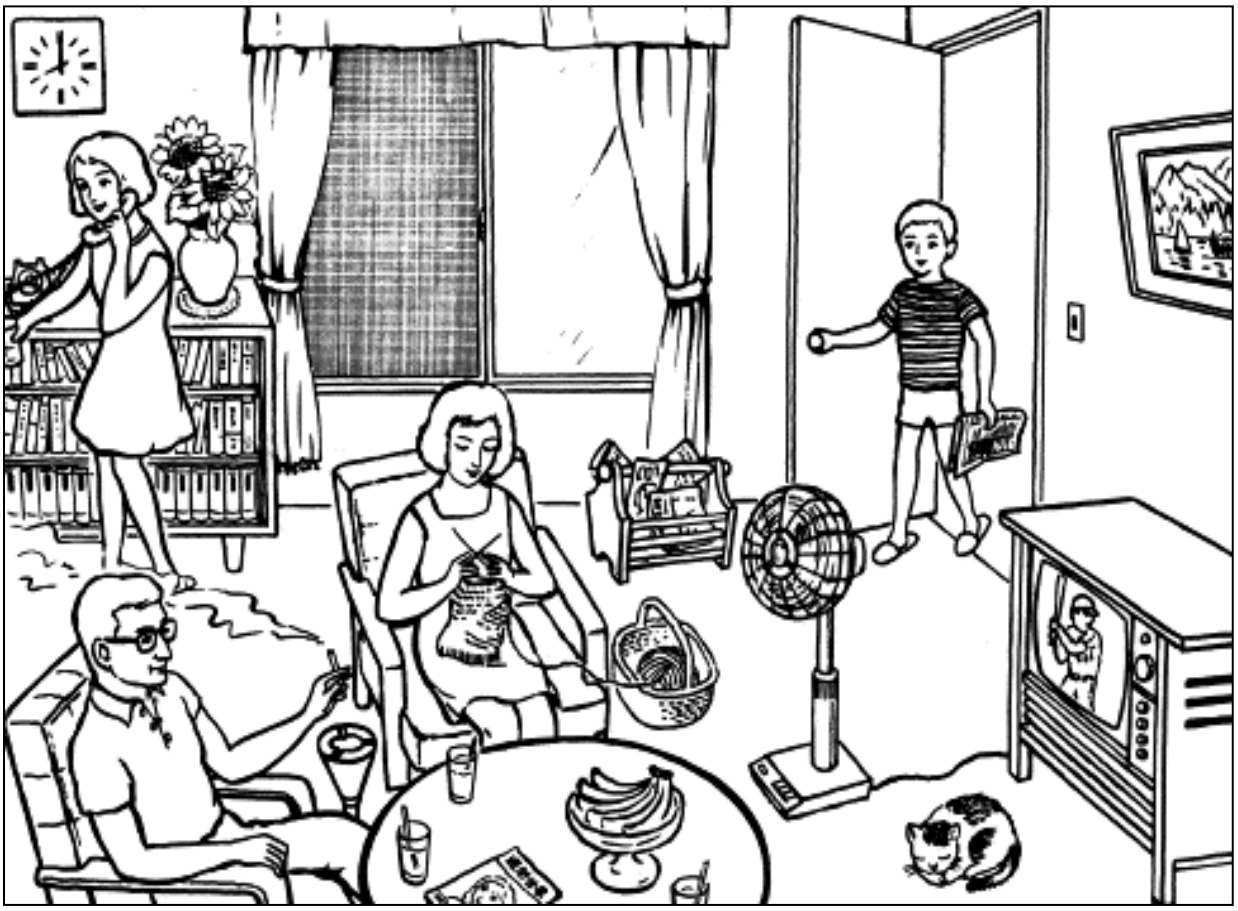

Figure B-1. An example of the standard picture of the MAPDS test

APPENDIX C
WORKING MEMORY TRAINING SYSTEM

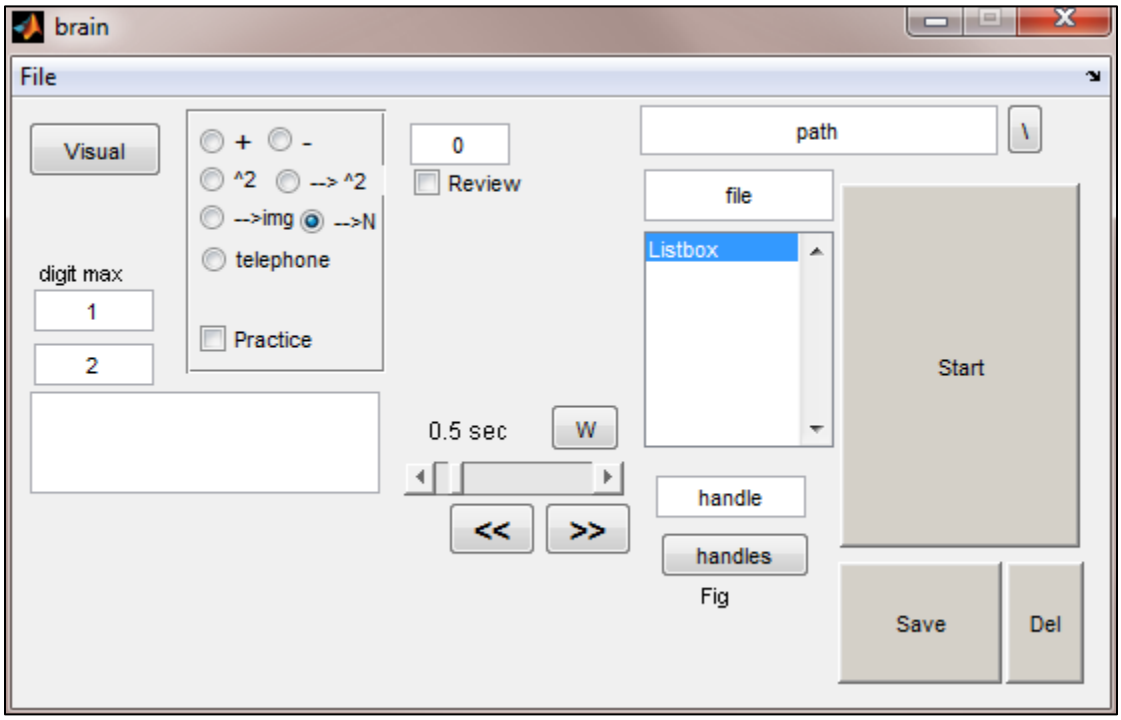

Figure C-1. Main page

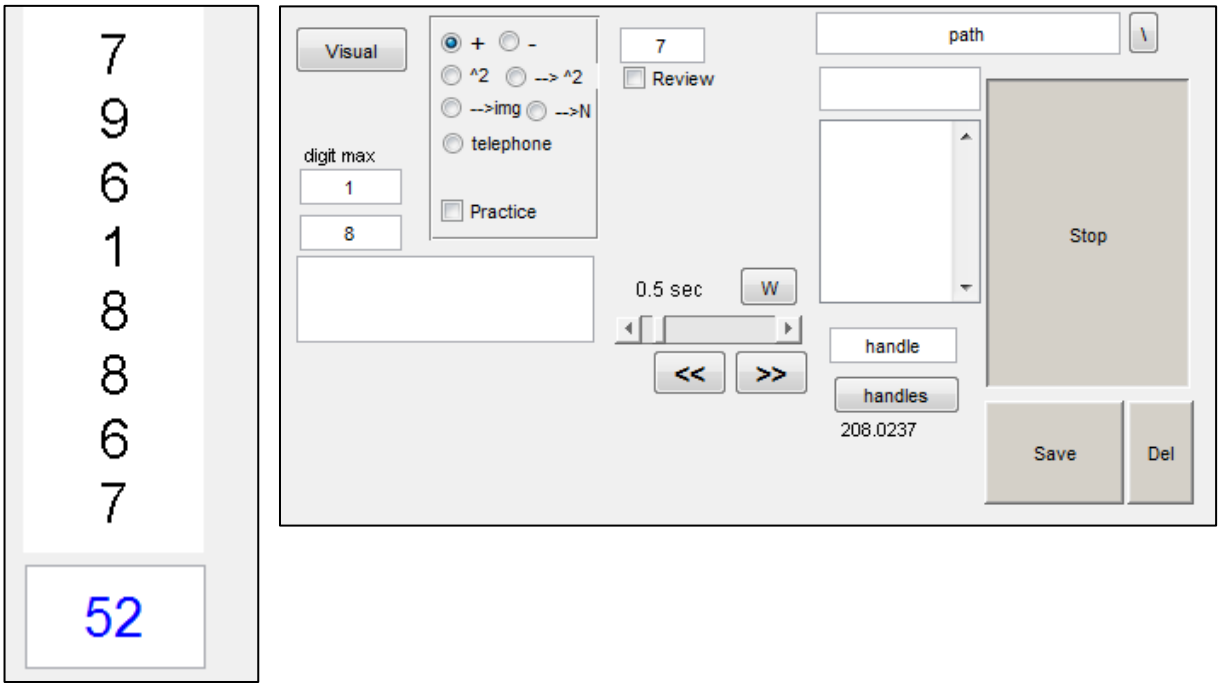

Figure C-2. Mental arithmetic training mode

Figure C-3. Image-numeric association practice mode

LIST OF REFERENCES

Adrian, E. D., and B. H. Matthews. (1934). The interpretation of potential waves in the cortex. J Physiol 81:440–71.

Akaike, H. (1974). New Look at Statistical-Model Identification. Ieee Transactions on Automatic Control AC19:716–723.

Aldenkamp AP, Alpherts WCJ, Sandstedt P, et al (1998) Antiepileptic drug-related cognitive complaints in seizure-free children with epilepsy before and after drug discontinuation. Epilepsia 39:1070–4.

Aldenkamp AP, Baker G, Mulder OG, Chadwick D, Cooper P, Doelman J, et al. (2000) A multicenter, randomized clinical study to evaluate the effect on cognitive function of topiramate compared with valproate as add-on therapy to carbamazepine in patients with partial-onset seizures. Epilepsia 41:1167–78.

Aldenkamp AP, Baker G, Mulder OG, et al. (2000) A multicenter, randomized clinical study to evaluate the effect on cognitive function of topiramate compared with valproate as add-on therapy to carbamazepine in patients with partial-onset seizures. Epilepsia 41: 1167–78.

Aldenkamp AP, Bodde N (2005) Behaviour, cognition and epilepsy. Acta Neurol Scand Suppl 182:19–25.

Aldenkamp AP. (2000) Cognitive effects of topiramate, gabapentin, and lamotrigine in healthy young adults. Neurology 54:271–2.

Aldenkamp AP. (2001) Effects of antiepileptic drugs on cognition. Epilepsia 42(suppl 1):46–49, discussion 40–41.

Algren, E., C. Boujon, J. Clarke, and C. Wang. (2002). Rapid distributed fronto-parieto-occipital processing stages during working memory in humans. Cerebral Cortex 12:710–728.

Atkinson, R.C., and R.M. Shiffrin. 1968. Human memory: A proposed system and its control processes. In The psychology of learning and motivation. London: Academic Press.

Baddeley, A., and S. Della Sala. (1996). Working memory and executive control. Philos Trans R Soc Lond B Biol Sci 351:1397–403; discussion 1403–4.

Baddeley, A., S. Gathercole, and C. Papagno. (1998). The phonological loop as a language learning device. Psychol Rev 105:158–73.

Berger, H. (1929). Über das elektroencephalogramm des menschen (On the electroencephalogram of man). Arch Psychiatr Nervenkr 87: 527–570.

Berti S, Roeber U, Schroger E (2004) Bottom-up influences on working memory: Behavioral and electrophysiological distraction varies with distractor strength. Experimental Psychology 51:249–257

Bootsma, HPR (2004) Topiramate in clinical practice: long-term experience in patients with refractory epilepsy referred to a tertiary epilepsy center. Epilepsy & Behavior 5:380–387

Braver TS, Cohen JD (2002) On the control of control: the role of dopamine in regulating prefrontal function and working memory. Control of cognitive processes: attention and performance XVIII. Cambridge, MA MIT Press:713–37.

Brovelli, A., M. Ding, A. Ledberg, Y. Chen, R. Nakamura, and S. L. Bressler. (2004). Beta oscillations in a large-scale sensorimotor cortical network: directional influences revealed by Granger causality. Proc Natl Acad Sci U S A 101 26:9849–54.

Busch, N. A., and C. S. Herrmann. (2003). Object-load and feature-load modulate EEG in a short-term memory task. Neuroreport 14:1721–4.

Chen, Y., S. L. Bressler, and M. Ding. (2006). Frequency decomposition of conditional Granger causality and application to multivariate neural field potential data. J Neurosci Methods 150:228–37.

Chen, Y., S. L. Bressler, K. H. Knuth, W. A. Truccolo, and M. Ding. (2006). Stochastic modeling of neurobiological time series: power, coherence, Granger causality, and separation of evoked responses from ongoing activity. Chaos 16:026113.

Colello RJ, Pott U, Schwab ME (1994) The role of oligodendrocytes and myelin on axon maturation in the developing rat retinofugal pathway. J Neurosci 14:2594 Y 605

Cooper, N. R., R. J. Croft, S. J. J. Dominey, A. P. Burgess, and J. H. Gruzelier. (2003). Paradox lost? exploring the role of alpha oscillations during externally vs. internally directed attention and the implications for idling and inhibition hypotheses. International Journal of Psychophysiology 47:65–74.

Coulter DA, Sombati S, DeLorenzo RJ (1993) Selective effects of topiramate on sustained repetitive firing and spontaneous bursting in cultured hippocampal neurons. Epilepsia 34(Suppl 2):123.

Curran T (2000). Brain potentials of recollection and familiarity. Memory & Cognition 28:923–938.

Curran T (2007) The FN400 indexes familiarity-based recognition of faces. Neuroimage 6:464–471

Devinsky O. (1995) Cognitive and behavioral effects of antiepileptic drugs. Epilepsia 36(suppl 2):S46 –S65. 3.

Ding, M. , Y. Chen, and S.L. Bressler. (2006). Granger causality: Basic theory and application to neuroscience. In Handbook of Time Series Analysis: Berlin:WILEY-VCH Verlag.

Ding, M., S. L. Bressler, W. Yang, and H. Liang. (2000). Short-window spectral analysis of cortical event-related potentials by adaptive multivariate autoregressive modeling: data preprocessing, model validation, and variability assessment. Biol Cybern 83:35–45.

Dodrill C (1988) Effects of antiepileptic drugs on abilities. J Clin Psychiatry 49(Suppl. 1):31–4.

Efron, B. (1982). The Jackknife, the Bootstrap, and Other Resampling Plans. Philadelphia: SIAM Press.

Enoch M, White KV, Harris CR, Rohrbaugh JW, Goldman D (2002)The relationship between two intermediate phenotypes for alcoholism:low voltage alpha EEG and low P300 ERP amplitude. Journal of Studies on Alcohol 63:i5 p509(9).

Ferree T (2006) Spherical splines and average referencing in scalp electroencephalography. Brain Topography 19:43–52.

Geweke, J. (1982). Measurement of linear-dependence and feedback between multiple time-series. Journal of the American Statistical Association 77:304–313.

Gibbs, JW; Sombati, S; DeLorenzo, RJ, et al. (2000) Cellular Actions of Topiramate: Blockade of Kainate-Evoked Inward Currents in Cultured Hippocampal Neurons. Epilepsia 41:S10–S16.

Granger, C. W. J. (1969). Investigating Causal Relations by Econometric Models and Cross-Spectral Methods. Econometrica 37:414–&.

Herrero AI, Del Olmo N, et al. (2002) Two new actions of topiramate: inhibition of depolarizing GABA(A)-mediated responses and activation of a potassium conductance. Neuropharmacology 42:210–220

Jensen, O., J. Gelfand, J. Kounios, and J. E. Lisman. (2002). Oscillations in the alpha band (9–12 Hz) increase with memory load during retention in a short-term memory task. Cerebral Cortex 12:877–882.

Kida E, Palminiello S, Golabek AA, Walus M, Wierzba-Bobrowicz T, Rabe A, et al. (2006) Carbonic anhydrase II in the developing and adult human brain. J Neuropathol Exp Neurol 65:664–674.

Klimesch, W. (1996). Memory processes, brain oscillations and EEG synchronization. International Journal of Psychophysiology 24:61–100.

Klimesch, W., P. Sauseng, and S. Hanslmayr. (2007). EEG alpha oscillations: The inhibition-timing hypothesis. Brain Research Reviews 53:63–88.

Klinger, E., K. C. Gregoire, and S. G. Barta. (1973). Physiological correlates of mental activity: eye movements, alpha, and heart rate during imagining, suppression, concentration, search, and choice. Psychophysiology 10:471–7.

Langtry HD, Gillis JC, Davis R (1997) Topiramate. A review of its pharmacodynamic and pharmacokinetic properties and clinical efficacy in the management of epilepsy. Drugs 54:752–73.

Lee S, Sziklas V, Andermann F, et al. (2003) The effects of adjunctive topiramate on cognitive function in patients with epilepsy. Epilepsia 44:339–47.

Loring DW, Marino S, Meador KJ (2007) Neuropsychological and behavioral effects of antiepilepsy drugs. Neuropsychol Rev 17:413–425.

Lutkepohl, H. (1993). Introduction To Multiple Time Series Analysis. New York: Springer.

Marciani MG, Spanedda F, Mattia D (1999) Neurophysiologic and neuropsychologic profiles of lamotrigine in epilepsy. Clin Neuropharmacol 22:159–163.

Martin R, Kuzniecky R, Ho S, et al. (1999) Cognitive effects of topiramate, gabapentin, and lamotrigine in healthy young adults. Neurology 52:321–7.

Martin R, Kuzniecky R, Ho S, et al. (1999) Cognitive effects of topiramate, gabapentin, and lamotrigine in healthy young adults. Neurology 52:321–7.

Martin R, Kuzniecky R, Ho S, Hetherington H, Pan J, Sinclair K, Gilliam F, Faught E (1999) Cognitive effects of topiramate, gabapentin, and lamotrigine in healthy young adults. Neurology 52:321–7.

Massagli TL. (1991) Neurobehavioral effects of phenytoin, carbamazepine, and valproic acid: implications for use in traumatic brain injury. Arch Phys Med Rehabil 72:219 –26.

McEvoy LK, Smith ME, Gevins A. (2001) Neuophysiological signals of working memory in normal aging. Cog Brain Res 11:363–76.

Meador K, Loring D, Allen M, et al. (1991) Comparative cognitive effects of carbamazepine and phenytoin in healthy adults. Neuology 41:1537–40.

Meador K, Loring D, Moore E, et al. (1995) Comparative cognitive effects of phenobarbital, phenytoin, and valproate in healthy adults. Neurology 45:1494–9.

Meador K, Loring D, Ray P, et al. (2001) Differential cognitive and behavioral effects of carbamazepine and lamotrigine. Neurology 56:1177–82.

Meador KJ (1997) Assessing cognitive effects of a new AED without the bias of practice effects. Epilepsia 38(suppl 3):S60.

Meador KJ, Gevins A, Loring DW, McEvoy LK, Ray PG, Smith ME, et al. (2007) Neuropsychological and neurophysiologic effects of carbamazepine and levetiracetam. Neurology 69:2076–2084.

Meador KJ, Gilliam FG, Kanner AM, et al. (2001) Cognitive and behavioral effects of antiepileptic drugs. Epilepsy Behav 2:SS1–SS17.

Meador KJ, Loring D, Vahle V, et al. (2005) Cognitive and behavioural effects of topiramate and lamotrigine in healthy volunteers. Neurology 64:2108–14.

Meador KJ, Loring DW, Moore EE, et al.(1995) Comparative cognitive effects of phenobarbital, phenytoin, and valproate in healthy adults. Neurology 45:1494 –9.

Meador KJ, Loring DW, Vahle VJ, et al. (2005) Cognitive and behavioral effects of lamotrigine and topiramate in healthy volunteers. Neurology 64:2108–2114.

Meador, Kimford J (1998) Cognitive and behavioral assessments in AED trials. Advances in Neurology; Antiepileptic drug development. 76: 231–238

Mecarelli, O; Piacenti, A; Pulitano, P, et al. (2001) Clinical and electroencephalographic effects of topiramate in patients with epilepsy and healthy volunteers. CLINICAL NEUROPHARMACOLOGY 24:284–289

Miller, G. A. (1956). The Magical Number 7, Plus or Minus 2— Some Limits on Our Capacity for Processing Information. Psychological Review 63:81–97.

Mima, T., T. Oluwatimilehin, T. Hiraoka, and M. Hallett. (2001). Transient interhemispheric neuronal synchrony correlates with object recognition. Journal of Neuroscience 21:3942–3948.

Mitra, P. P., and B. Pesaran. (1999). Analysis of dynamic brain imaging data. Biophysical Journal 76 (2):691–708.

Neurosurg Psychiary 69:636–41.

Nunez PL, Srinivasan R, Westdorp AF, Wijesinghe RS, Tucker DM, Silberstein RB, Cadusch PJ (1997) EEG coherency.1: statistics, reference electrode, volume conduction, Laplacians, cortical imaging, and interpretation at multiple scales. Electroencephalography and Clinical Neurophysiology 103:499–515.

Ojemann LM, Crawford CA, Dodrill CB, et al. (1999) Language disturbances as a side effect of topiramate and zonisamide therapy. Epilepsia 40:66–66

Palva, J. M., S. Palva, and K. Kaila. (2005). Phase synchrony among neuronal oscillations in the human cortex. Journal of Neuroscience 25:3962–3972.

Palva, S., and J. M. Palva. (2007). New vistas for alpha-frequency band oscillations. Trends in Neurosciences 30:150–158.

Palva, S., K. Linkenkaer-Hansen, R. Naatanen, and J. M. Palva. (2005). Early neural correlates of conscious somatosensory perception. Journal of Neuroscience 25:5248–5258.

Park SP, Kwon OY (2009) Increased EEG Current-Source Density in the High Beta Frequency Band Induced by Levetiracetam Adjunctive Therapy in Refractory Partial Epilepsy. JOURNAL OF CLINICAL NEUROLOGY 5:178–185

Peterson, L. R., and M. J. Peterson. (1959). Short-term retention of individual verbal items. J Exp Psychol 58:193–8.

Pfurtscheller, G. (2001). Functional brain imaging based on ERD/ERS. Vision Research 41:1257–1260.

Pfurtscheller, G. (2003). Induced oscillations in the alpha band: Functional meaning. Epilepsia 44:2–8.

Placidi F, Tombini M, Romigi A, et al. (2004) Topiramate: effect on EEG interictal abnormalities and background activity in patients affected by focal epilepsy. Epilepsy Res 58:43–52.

Placidi, F; Tombini, M; Romigi, A, et al. (2004) Topiramate: effect on EEG interictal abnormalities and background activity in patients affected by focal epilepsy 58:43–52

Polich J (2003) Theoretical overview of P3a and P3b. Detection of change: event-related potential and fMRI findings. Boston MA Kluwer Academic:83–98.

Polich J (2004) Clinical application of the P300 event-related brain potential, Phys Med Rehabil Clin North Am 15:133–61

Polich J, Kok A. (1995) Cognitive and biological determinants of P300: an integrative review. Biol Psychol 41:103–46.

Ray, W. J., and H. W. Cole. (1985). EEG activity during cognitive processing: influence of attentional factors. Int J Psychophysiol 3:43–8.

Ray, W. J., and H. W. Cole. (1985). EEG alpha-activity reflects attentional demands, and beta-activity reflects emotional and cognitive-processes. Science 228:750–752.

Roznowski M (1993) A note on some psychometric properties of sternberg task-performance. Intelligence 17:389–398

Rugg, M.D., Curran T (2007). Event-related potentials and recognition memory. Trends in Cognitive Science 11:251–257.

Salinsky M, Binder L, Storzbach D, Oken B. (2003) Assessment of CNS effects of antiepileptic drugs using quantitative EEG measures. Epilepsia 44:1042–50.

Salinsky M, Spencer D, Oken B, Storzbach D. (2004) Effects of oxcarbazepine and phenytoin on the EEG and cognition in healthy volunteers. Epilepsy Behav 5:894–902.

Salinsky M, Storzbach D, Binder L, Arons C, Dodrill C. (2002) Effects of gabapentin and carbamazepine on the EEG, alertness, and cognition in healthy volunteers. Epilepsia 43:482–90.

Salinsky M, Storzbach D, Oken B, Spencer D. (2007) Topiramate effects on the EEG and alertness in healthy volunteers: A different profile of antiepileptic drug neurotoxicity. Epilepsy & Behavior 10:463–469

Salinsky MC, Binder LM, Oken BS, et al. (2002) Effects of gabapentin and carbamazepine on EEG and cognition in healthy volunteers. Epilepsia 43:482–490.

Sanchez I, Hassinger L, Sihag RK, et al. (2000) Local control of neurofilament accumulation during radial growth of myelinating axons in vivo. Selective role of site-specific phosphorylation. J Cell Biol 151:1013 Y 24

Sauseng, P., W. Klimesch, M. Doppelmayr, T. Pecherstorfer, R. Freunberger, and S. Hanslmayr. (2005). EEG alpha synchronization and functional coupling during top-down processing in a working memory task. Human Brain Mapping 26:148–155.

Schack B, Klimesch W, Sauseng P. (2005) Phase synchronization between theta and upper alpha oscillations in a working memory task. Int J Psychophysiol 57:105–14.

Schupp, H. T., W. Lutzenberger, N. Birbaumer, W. Miltner, and C. Braun. (1994). Neurophysiological differences between perception and imagery. Brain Res Cogn Brain Res 2:77–86.

Schwarz, G. (1978). Estimating Dimension of a Model. Annals of Statistics 6:461–464.

Shank RP, Gardocki JF, Vaught JL, Davis CB, Schupsky JJ, Raffa RB, Dodgson SJ, Nortey SO, Maryanoff BE (1994) Topiramate: Preclinical evaluation of a structurally novel anticonvulsant. Epilepsia 35:450–60.

Shank RP, Gardocki JF, Vaught JL, Davis CB, Schupsky JJ, Raffa RB, Dodgson SJ, Nortey SO, Maryanoff BE (1994) Topiramate: Preclinical evaluation of a structurally novel anticonvulsant. Epilepsia 35:450–60.

Shank, RP; Gardocki, JF; Streeter, AJ, et al. (2000) An overview of the preclinical aspects of topiramate: Pharmacology, pharmacokinetics, and mechanism of action EPILEPSIA 41:S3–S9

Shaw, J.C. (2003). The Brain's Alpha Rhythms and the Mind, Elsevier, Amsterdam.

Smith ME, Gevins A, McEvoy LK, Meador KJ, Ray PG, Gilliam F. (2006) Distinct cognitive neurophysiologic profiles for lamotrigine and topiramate. Epilepsia 47:695–703.

Sternberg.S. (1966). High-Speed Scanning in Human Memory. Science 153:652–&. Thompson P, Baxendale S, Duncan J, Sander J. (2002) Effects of topiramate on cognitive function. J Neurol

Taverna S, Sancini G, Mantegazza M, et al. (1999) Inhibition of transient and persistent Na+ current fractions by the new anticonvulsant topiramate Journal of Pharmacology and Experimental Therapeutics 288:960–968

Veauthier J, Haettig H, Meencke HJ (2009) Impact of levetiracetam add-on therapy on different EEG occipital frequencies in epileptic patients. Seizure 18:392–395.

Vermeulen J, Aldenkamp AP. (1995) Cognitive side-effects of chronic antiepileptic drug treatment: a review of 25 years of research. Epilepsy Res 22:65–95.

von Stein, A., C. Chiang, and P. Konig. (2000). Top-down processing mediated by interareal synchronization. Proceedings of the National Academy of Sciences of the United States of America 97:14748–14753.

Voss JL, Federmeier KD (2010) FN400 potentials are functionally identical to N400 potentials and reflect semantic processing during recognition testing. Psychophysiology 1–15.

White SH, Brown BS, Woodhead JH, Skeen GA, Harold HW (1997) Topiramate enhances GABA-mediated chloride flux and GABA-evoked chloride currents in murine brain neurons and increases seizure threshold. Epilepsy Research 28:167–179

Wiener, N. 1956. The theory of prediction. In Modern Mathermatics for Engineers. New York: McGraw-Hill.

Wilkins A, Majed H, Layfield R, et al. (2003) Oligodendrocytes promote neuronal survival and axonal length by distinct intracellular mechanisms: A novel role for oligodendrocyte-derived glial cell line-derived neurotrophic factor. J Neurosci 23:4967 Y 74

Zona C, Ciotti MT, Avoli M (1997) Topiramate attenuates voltage-gated sodium currents in rat cerebellar granule cells. Neuroscience Letters 231:123-126

BIOGRAPHICAL SKETCH

Sahng-Min Han was born on a beautiful national holiday in Seoul, Republic of Korea. The younger of two children, he grew up mostly in Daejeon, Korea, graduating from Daedeok High School located in Daedeok Science Town in 1994. He earned his Bachelor of Engineering in electrical engineering at Chungnam National University in 1999. Upon graduation, Sahng-Min joined the active duty Republic of Korea Air Force and received a commission as a 2nd Lieutenant in 2000. As an Interpreting and Translating Officer, he worked closely with U.S. 7th Air Force Officers in the Republic of Korea Air Operations Command where he learned the importance of the strong ROK-U.S. strategic alliance through numerous Joint and Combined Operations to provide stability and security for Far East Asia against potential communist threats. Sahng-Min's military mission as an officer has afforded him many wonderful opportunities; teaching cadets as an Instructor in ROK Air Force Academy, publishing Air Strategy and Air Review in Air University and selection to the delegates of the 2002 Fédération Internationale de Football Association (FIFA) World Cup, where he worked as an Intellectual Property Specialist. Official commendations by the Minister of National Defense and by the Commandant of Air University were awarded to him before he was discharged in 2003. He came to United States of America in the fall of 2003 and began his graduate study with the Department of Electrical and Computer Engineering at the University of Florida. He earned his master's degree in 2005. He continued his study toward his Ph.D. with Dr. Mingzhou Ding in J. Crayton Pruitt Family Department of Biomedical Engineering.